




ORIGINAL RESEARCH

C1q/Tumor Necrosis Factor–Related Protein-9 Is a Novel Vasculoprotective Cytokine That Restores High Glucose-Suppressed Endothelial Progenitor Cell Functions by Activating the Endothelial Nitric Oxide Synthase

Qingsong Hu , MD, PhD*; Wan Qu, MS*; Tao Zhang, MD; Jianyi Feng, MS; Xiaobian Dong, MD; Ruqiong Nie, MD, PhD; Junyu Chen, MS; Xiaoqing Wang, MS; Changnong Peng , MS; Xiao Ke , MD, PhD

BACKGROUND: This study investigated whether gCTRP9 (globular C1q/tumor necrosis factor–related protein-9) could restore high-glucose (HG)-suppressed endothelial progenitor cell (EPC) functions by activating the endothelial nitric oxide synthase (eNOS).

METHODS AND RESULTS: EPCs were treated with HG (25 mmol/L) and gCTRP9. Migration, adhesion, and tube formation assays were performed. Adiponectin receptor 1, adiponectin receptor 2, and N-cadherin expression and AMP-activated protein kinase, protein kinase B, and eNOS phosphorylation were measured by Western blotting. eNOS activity was determined using nitrite production measurement. In vivo reendothelialization and EPC homing assays were performed using Evans blue and immunofluorescence in mice. Treatment with gCTRP9 at physiological levels enhanced migration, adhesion, and tube formation of EPCs. gCTRP9 upregulated the phosphorylation of AMP-activated protein kinase, protein kinase B, and eNOS and increased nitrite production in a concentration-dependent manner. Exposure of EPCs to HG-attenuated EPC functions induced cellular senescence and decreased eNOS activity and nitric oxide synthesis; the effects of HG were reversed by gCTRP9. Protein kinase B knockdown inhibited eNOS phosphorylation but did not affect gCTRP9-induced AMP-activated protein kinase phosphorylation. HG impaired N-cadherin expression, but treatment with gCTRP9 restored N-cadherin expression after HG stimulation. gCTRP9 restored HG-impaired EPC functions through both adiponectin receptor 1 and N-cadherin-mediated AMP-activated protein kinase /protein kinase B/eNOS signaling. Nude mice that received EPCs treated with gCTRP9 under HG medium showed a significant enhancement of the reendothelialization capacity compared with those with EPCs incubated under HG conditions.

CONCLUSIONS: CTRP9 promotes EPC migration, adhesion, and tube formation and restores these functions under HG conditions through eNOS-mediated signaling mechanisms. Therefore, CTRP9 modulation could eventually be used for vascular healing after injury.

Key Words: C1q/TNF-related protein-9 ■ diabetes ■ endothelial nitric oxide synthase (eNOS) ■ endothelial progenitor cells ■ high glucose ■ reendothelialization

Correspondence to: Changnong Peng, MS and Xiao Ke, MD, PhD, Department of Cardiology, Fuwai Hospital, Chinese Academy of Medical Sciences (Shenzhen Sun Yat-Sen Cardiovascular Hospital), Shenzhen 518057, China. Email: pengchangnong1965@163.com; xiaokehospital@126.com

*Q. Hu and W. Qu contributed equally.

This manuscript was sent to Julie K. Freed, MD, PhD, Associate Editor, for review by expert referees, editorial decision, and final disposition.

Supplemental Material is available at <https://www.ahajournals.org/doi/suppl/10.1161/JAHA.123.030054>

For Sources of Funding and Disclosures, see page 17.

© 2024 The Authors. Published on behalf of the American Heart Association, Inc., by Wiley. This is an open access article under the terms of the [Creative Commons Attribution-NonCommercial-NoDerivs](https://creativecommons.org/licenses/by-nc-nd/4.0/) License, which permits use and distribution in any medium, provided the original work is properly cited, the use is non-commercial and no modifications or adaptations are made.

JAHA is available at: www.ahajournals.org/journal/jaha

RESEARCH PERSPECTIVE

What Is New?

- C1q/tumor necrosis factor–related protein-9 restores high-glucose–suppressed endothelial progenitor cells in vitro functions, including migration, adhesion, and vasculogenesis.
- C1q/tumor necrosis factor–related protein-9 restores high-glucose–suppressed endothelial progenitor cells through adiponectin receptor 1 and N-cadherin–mediated AMP-activated protein kinase/protein kinase B/endothelial nitric oxide synthase signaling pathways.

What Question Should be Addressed Next?

- Further studies are needed to refine the study of C1q/tumor necrosis factor–related protein-9 on diabetes-induced vascular injury in vivo and focus on endothelial nitric oxide synthase for C1q/tumor necrosis factor–related protein-9 in the regulation of endothelium repair and the progression of vascular remodeling.

Nonstandard Abbreviations and Acronyms

adipoR1	adiponectin receptor 1
adipoR2	adiponectin receptor 2
Akt	protein kinase B
AMPK	AMP-activated protein kinase
CTRP	C1q/tumor necrosis factor–related protein
eNOS	endothelial nitric oxide synthase
EPC	endothelial progenitor cell
gCTRP9	globular C1q/tumor necrosis factor–related protein-9
HG	high-glucose
L-NAME	N(ω)-nitro-L-arginine methyl ester
NO	nitric oxide
PBMNCs	peripheral blood mononuclear cells
P-Akt	phosphorylated protein kinase B
P-eNOS	phosphorylated endothelial nitric oxide synthase
siRNA	small inhibitory RNA
α-SMA	α-smooth muscle actin

Macro- and microvascular lesions and injuries are the primary causes of morbidity and death among people with diabetes.¹ Hyperglycemia plays a crucial role in the development of macro- and

microvascular complications in individuals with type 2 diabetes.² This condition induces endothelial dysfunction, which is the main initiating factor of vascular diseases.³ Thus, interventions that can restore endothelial function are beneficial for the prognosis of patients with type 2 diabetes.

Available evidence supports the notion that circulating endothelial progenitor cells (EPCs) play important roles in endothelial recovery and maintaining endothelial integrity after injury or damage, which accelerates reendothelialization and protects against atherosclerosis.^{4–8} The number of EPCs in circulation reflects the capacity for vascular repair.⁹ However, clinical and animal studies have demonstrated that individuals with type 2 diabetes have decreased numbers of EPCs in circulation and that injured EPC functions contribute to a vicious cycle of endothelial dysfunction and atherosclerosis progression.^{10,11} Nitric oxide (NO)-mediated mechanisms are involved in the attenuation of human EPC functions after long-term exposure to high glucose (HG).¹² Therefore, strategies for type 2 diabetes could be designed to improve EPC functions by enhancing NO bioavailability.

CTRPs (C1q/tumor necrosis factor–related proteins) are conserved paralogs of adiponectin and consist of a collagen domain and a C-terminal globular C1q domain.^{13,14} Among the CTRPs, CTRP9 is a secreted glycoprotein that is highly expressed in blood vessels and has antiatherogenic effects.¹⁵ CTRP9 promotes endothelial cell functions and endothelium-dependent vasodilation,¹⁶ and its injection attenuates neointima formation in response to vascular injury.¹⁷ Additionally, CTRP9 overexpression reduces atherogenesis in high-fat-fed apoE-KO mice.¹⁸ Plasma CTRP9 levels are decreased in individuals with type 2 diabetes¹⁹ and are associated with atherosclerotic cardiovascular disease events.²⁰ Furthermore, gCTRP9 (globular CTRP9) can increase endothelial NO-related neovascularization and suppress excess reactive oxidative stress under HG conditions.^{21,22}

Endothelial dysfunction is influenced by several factors. AMPK (AMP-activated protein kinase) is a sensor of the cell's energy status and helps maintain energy balance.^{23,24} In endothelial cells, AMPK regulates vascular functions by activating the AMPK/Akt (protein kinase B)/endothelial nitric oxide synthase (eNOS) pathway to stimulate NO production and vasodilation.^{25–27} Type 2 diabetes and obesity lead to dysfunctional AMPK, which contributes to endothelial dysfunction.^{27,28} Adiponectin receptor 1 (adipoR1) mediates the beneficial effects of adiponectin on blood vessels by participating in NO release through eNOS activation and vasodilation.²⁹ N-cadherin mediates cell–cell interactions between endothelial cells and smooth muscle cells in the blood vessel wall and is crucial for cell recruitment during angiogenesis and vascular repair.³⁰

Therefore, CTRP9 may have beneficial effects on EPCs for vascular repair, but it is unknown whether gCTRP9 can enhance impaired EPC functions induced by HG and whether this enhancement could involve AMPK/Akt/eNOS, adipoR1, and N-cadherin. The present study investigates whether the administration of gCTRP9 can restore HG-suppressed EPC functions by activating eNOS.

METHODS

The data that support the findings of this study are available from the corresponding author upon reasonable request.

Isolation Characterization of Human Late EPCs

This study was approved by the Ethics Committee of First Affiliated Hospital of Jinan University. All donors provided written informed consent. Human late EPCs were purified from 20 healthy individuals and cultured following previously described methods.³¹ Briefly, peripheral blood mononuclear cells (PBMNCs) were maintained in endothelial cell basal medium-2 (Lonza, Basel, Switzerland) supplemented with endothelial growth medium-SingleQuots (Clonetics, San Diego, CA) in fibronectin-coated 6-well plates. After 4 days of culture, nonadherent cells were removed. The adherent cells were cultured for 28 days, with the medium being refreshed every 7 days. After 28 days of culture, human late EPCs were characterized by a double-positivity for BS-1 lectin binding (0.01 mg/mL; Sigma-Aldrich, St. Louis, MO) and Dil-acetylated low-density lipoprotein uptake (0.02 mg/mL; Invitrogen, Carlsbad, CA). Cultured EPCs were incubated with 1,1'-dioctadecyl-3,3,3',3'-tetramethylindocarbocyanine-acetylated low-density lipoprotein for 2 hours in a cell incubator. Subsequently, cells were washed and fixed with 4% paraformaldehyde for 15 minutes and incubated with FITC-BS-1 lectin for 1 hour. Plates of cells were again washed and incubated with DAPI nuclear counterstain. Double-positive cells were observed with a fluorescent microscope ($\times 200$ magnification; Olympus, Tokyo, Japan).

Flow Cytometry Analysis

EPCs marker proteins were examined by flow cytometry analysis using CD31 (endothelial marker) (12.5 $\mu\text{g/mL}$; Pharmingen, BD Biosciences, Franklin Lakes, NJ), kinase-insert domain receptor (endothelial marker) (50 $\mu\text{g/mL}$; R&D Systems, Minneapolis, MN), CD34 (stem cell marker) (250 $\mu\text{g/mL}$; BD Pharmingen, San Diego, CA), CD133 (stem cell marker) (250 $\mu\text{g/mL}$; BD Pharmingen), CD14 (monocytes marker) (50 $\mu\text{g/mL}$;

mL; BD Pharmingen), and CD45 (leukocyte marker) (50 $\mu\text{g/mL}$; BD Pharmingen). To determine the expression of each of these surface antigens, cells were incubated for 40 minutes at 4 °C in a volume of 100 μL with an appropriate amount of antibody or corresponding IgG isotype control. At least 1×10^5 EPCs were acquired using flow cytometry (Beckman-Coulter, Fullerton, CA).

Measurement of Cytokine Concentration of Cell Supernatant

For 10 and 28 days, 1×10^6 cells were incubated with endothelial cell basal medium-2, and the supernatant was harvested. The cytokine concentration was measured with vascular endothelial growth factor (VEGF; No. DVE00, R&D Systems), interleukin-8 (No. D8000C, R&D Systems) and stromal cell-derived factor 1 (No. DSA00, R&D Systems) Quantikine ELISA kit.

Experimental Cell Groups

The cells were grouped as (1) late EPCs treated with gCTRP9 (0.5–10 $\mu\text{g/mL}$; Aviscera Bioscience, Santa Clara, CA) for 2 or 24 hours under a “healthy” environment; (2) late EPCs incubated with HG (25 mmol/L) or mannitol (25 mmol/L) for 4 days; (3) late EPCs incubated with HG (25 mmol/L) for 4 days and then continually treated with gCTRP9 (0.5–10 $\mu\text{g/mL}$) for 2 or 24 hours after the 4 days of HG; and (4) late EPCs incubated with HG (25 mmol/L) for 4 days and then continually treated with or without gCTRP9 (5 $\mu\text{g/mL}$) for 24 hours after the 4 days of HG in the presence or absence of N(ω)-nitro-L-arginine methyl ester (L-NAME; 100 $\mu\text{mol/L}$; Sigma-Aldrich); (5) late EPCs incubated with HG (25 mmol/L) for 4 days and then continually treated with or without gCTRP9 (5 $\mu\text{g/mL}$) for 24 hours after the 4 days of HG in the presence or absence of sodium nitroprusside (100 $\mu\text{mol/L}$; Sigma-Aldrich); (6) late EPCs incubated with HG (25 mmol/L) for 4 days and then continually treated with or without gCTRP9 (5 $\mu\text{g/mL}$) for 24 hours after the 4 days of HG in the presence or absence of eNOS small inhibitory RNA (siRNA; 25 nmol/L or 50 nmol/L); (7) late EPCs incubated with HG (25 mmol/L) for 4 days and continually treated with or without gCTRP9 (5 $\mu\text{g/mL}$) for 24 hours in the presence or absence of Compound C (AMPK inhibitor) (1–10 $\mu\text{mol/L}$; Merck Frosst, Montreal, Canada) or LY294002 (Akt inhibitor) (1–10 $\mu\text{mol/L}$; Merck Frosst); and (8) late EPCs incubated with HG (25 mmol/L) for 4 days and continually treated with or without gCTRP9 (5 $\mu\text{g/mL}$) for 24 hours in the presence or absence of adipoR1 siRNA (50 nmol/L), adiponectin receptor 2 (adipoR2) siRNA (50 nmol/L) or N-cadherin siRNA (50 nmol/L).

EPC Migration Assay

The migratory capability of the EPCs was evaluated using a modified Boyden chamber assay. The EPCs were digested with trypsin/EDTA, resuspended (4×10^4) in 250 μ L of endothelial cell basal medium-2, and added to the upper chambers (8- μ m pore size) of a modified Boyden chamber (Corning Inc., Corning, NY). The chamber was placed in a 24-well plate containing endothelial cell basal medium-2 (500 μ L) with 50 ng/mL VEGF (Peprotech, Rocky Hill, NJ). After 24 hours, the membrane was washed with PBS and fixed with 4% paraformaldehyde. The upper side of the membrane was wiped gently. The lower chamber was stained with crystal violet for 30 minutes. The number of migrating cells was counted from 5 randomly selected fields under light microscopy by an independent blinded researcher.

Fibronectin Adhesion Assay

The EPC fibronectin adhesion test was performed as previously described.³² Human late EPCs (1×10^5) were seeded on fibronectin (100 μ g/mL)-coated 24-well plates in endothelial cell growth medium-2 and incubated for 30 minutes at 37 °C. Nonadherent cells were removed by washing twice with PBS. Adherent cells were photographed with high-power fields under an inverted fluorescent microscope at $\times 200$ magnification and were counted from 5 randomly selected fields by an independent blinded researcher.

Tube Formation Assay

The In Vitro Angiogenesis Assay Kit (BD Biosciences) was used to evaluate the EPC tube formation capacity, according to the manufacturer's instructions. Briefly, 48-well plates were coated with growth factor-reduced Matrix gel (150 μ L/well). EPCs were plated (5×10^4 cells/well) in 200 μ L culture medium and incubated at 37 °C with 5% CO₂ for 24 hours to form tubes. An inverted light microscope was used to examine tube formation. Five representative fields were photographed. The number of branch points was examined using Image-Pro Plus (Media Cybernetics, Inc., Rockville, MD).

Senescence Assay

Cell senescence was evaluated with a Senescence Cell Staining kit (Sigma), according to the manufacturer's instructions. Briefly, after washing with PBS, EPCs were fixed for 6 minutes in 2% formaldehyde and 0.2% glutaraldehyde in PBS and then incubated for 12 hours at 37 °C without CO₂ with a Senescence Cell Staining solution. After staining, cells were washed with PBS 3 times, and the number of senescent cells (in blue) was

counted from 5 randomly selected fields using a light microscope by an independent blinded investigator.

Western Blotting

Proteins were extracted from the cells using the RIPA buffer (Cell Signaling Technology, Danvers, MA), separated using SDS-PAGE, and transferred onto PVDF membranes. These membranes were incubated with rabbit anti-phospho-eNOS^{ser1177} (ab184154; 1:1000; Abcam, Cambridge, MA), rabbit anti-eNOS (ab300071; 1:1000; Abcam), rabbit anti-phospho-Akt^{ser473} (No. 4060; 1:1000; Cell Signaling Technology), rabbit anti-Akt (#9272; 1:1000; Cell Signaling Technology), rabbit anti-phospho-AMPK^{Thr172} (No. 50081; 1:1000; Cell Signaling Technology), rabbit anti-AMPK (#5832; 1:1000; Cell Signaling Technology), mouse anti-adipoR1 (sc-518030; 1:1000; Santa Cruz Biotechnology, Santa Cruz, CA), mouse anti-adipoR2 (sc-514045; 1:1000; Santa Cruz Biotechnology), rabbit anti-N-cadherin (ab76011; 1:1000; Abcam), and rabbit anti- β -actin (ab8227; 1:5000; Abcam) overnight at 4°C. The membranes were incubated with HRP-conjugated rabbit anti-IgG (1:2000; Cell Signaling Technology) or HRP-conjugated anti-mouse IgG (1:5000; Cell Signaling Technology). The proteins were visualized using an ECL chemiluminescence system (Cell Signaling Technology). The gray values of the bands were analyzed using ImageJ (National Institutes of Health, Bethesda, MD).

Nitrite Levels

After incubating late EPCs in different conditions and treatments for 4 days, the nitrite levels in the conditioned medium were measured using the Griess reagent (Beyotime Technology, Beijing, China), according to the manufacturer's instructions.

Silencing of eNOS, N-Cadherin, AdipoR1, and AdipoR2

siRNA against eNOS, N-cadherin, adipoR1, and adipoR2 were from Santa Cruz Biotechnology. The late EPCs were treated with 25 or 50 nmol/L siRNA. A scrambled siRNA (Santa Cruz Biotechnology) was used as control. Transfection was performed according to the manufacturer's protocol. The siRNA sequences were eNOS-siRNA-1, 5'-GCA GGU CUG CAC AGG AAA UTT-3'; eNOS-siRNA-2, 5'-AUU UCC UGU GCA GAC CUG CTT-3'; adipoR1-siRNA-1, 5'-GGA CAA CGA CUA UCU GCU ACA TT-3'; adipoR1-2, 5'-TGT AGC AGA TAG TCG TTG TCC TT-3'; adipoR2-1: 5'-GGA GUU UCG UUU CAU GAU CGG TT-3'; adipoR2-2, 5'-CCG ATC ATG AAA CGA AAC TCC TT-3'; N-cadherin-siRNA-1, 5'-GGC CAA ACA ACU UUU AAU U-3'; N-cadherin-siRNA-2, 5'-GGC UUC UGG

UGA AAU CGC A-3'. Western blotting was used to determine the interference efficiency.

Left Carotid Artery Injury Animal Model and In Vivo Reendothelialization Assay

The left carotid artery injury animal model was established as previously described^{6–8,31} (6–8 weeks old) (Laboratory Animal Center of Jinan University, Guangzhou, China). The protocol was approved by the Animal Care and Use Committees of Jinan University. The sample size was calculated using the *E*-value.³³ The mice were anesthetized using intraperitoneal 100 mg/kg ketamine and 5 mg/kg xylazine. The left carotid artery was exposed via a middle incision on the ventral side of the neck. The bifurcation of the carotid artery was located, and 2 ligatures were placed around the external carotid artery, which was tied off with a distal ligature. An incision was made between the ligatures to introduce the denudation device. A curved flexible wire (0.35-mm diameter) was introduced into the common carotid artery and passed over the lining of the artery 3 times to denude the endothelium. The wire was removed, and the external carotid artery was tied off proximal to the incision hole with a proximal ligature.

The EPCs were prelabeled with CM-Dil 3 hours before injection into the animal. The mice were randomized to 4 groups ($n=5$ /group) for tail vein injection of healthy EPCs, EPCs treated with HG for 4 days (HG+EPCs), EPCs treated with gCTRP9 5 μ g/mL for 24 hours (gCTRP9+EPCs), and EPCs treated with HG and gCTRP9 5 μ g/mL (24 hours followed by HG for 4 days) (gCTRP9+HG+EPCs). Then, 5×10^5 cells in 100 μ L of PBS were injected 3 hours after carotid artery injury according to grouping. After 5 days, the animals were euthanized using isoflurane anesthesia. The mice were transfused with 3% Evans blue dye 10 minutes before euthanasia to identify endothelial regeneration after modeling. After harvesting, the arteries were opened longitudinally and placed on slides. Pictures were taken using a microscope (MS5, Olympus, Tokyo, Japan). The arteries were harvested on day 5 and fixed in the Tissue-Tek O.C.T. compound (Sakura Finetek, Torrance, CA). Frozen sections were stained with DAPI. The CM-Dil-labeled EPCs (red cells) were detected using a fluorescence microscope (BX51, Olympus).

Immunohistochemistry

For the in vitro experiment, the EPCs were fixed with 4% paraformaldehyde and permeabilized in PBS with 0.1% Triton X-100 (Sigma) for 10 minutes. The cells were blocked with 1% BSA in PBS for 2 hours and incubated overnight (4 °C) with primary antibodies rabbit anti-human N-cadherin (ab76011; 1:100; Abcam) and rabbit anti-human CD31 (ab28364; 1:100; Abcam). The

primary antibodies were visualized with a secondary antibody conjugated with Alexa Fluor 488 or Alexa Fluor 633 (1:500; Molecular Probes, Eugene, OR). Nuclei were stained with DAPI. The cells were observed under a confocal microscope.

For the animal experiment, mouse normal arteries were harvested and fixed in the Tissue-Tek O.C.T. compound (Sakura Finetek). Frozen sections slides (10 μ m) were preincubated with 5% normal goat serum for 30 minutes, reacted with a rat anti-mouse CD31 (No. 550274; 1:200; BD Pharmingen), rabbit anti-mouse α -smooth muscle actin (α -SMA; ab5694; 1:200; Abcam), rabbit anti-mouse AdipoR1 (ab70362; 1:200; Abcam), anti-mouse adipoR2 (monoclonal antibody) (sc-514045; 1:200; Santa Cruz Biotechnology) and rabbit anti-mouse N-cadherin (ab76011; 1:100; Abcam) overnight, followed by Alexa Fluor 488 or Alexa Fluor 633-conjugated secondary antibody (1:500; Molecular Probes) for 1 hour at room temperature. Slides were washed 3 times with PBS with Tween 20 after each antibody incubation, for 10 minutes each time, and DAPI was used to stain the nuclei. The sections were observed under a confocal microscope.

Statistical Analysis

All data were presented as means \pm SEM. Unpaired Student's *t*-test or 1-way ANOVA followed by Bonferroni's multiple comparison tests were used to determine the statistical significance among treatment groups. Correlations between eNOS activity and nitrite production were analyzed using Pearson correlation analysis. All statistical analyses and graph plotting were carried out using GraphPad Prism 7.0 (GraphPad Software, La Jolla, CA).

RESULTS

Identification of Human Late EPCs

After seeding, the PBMNCs had a round shape (Figure S1A: a,b). After 3 to 7 days of culture, the cells attached and clustered with an elongated spindle shape (Figure S1A: c,d), as described by Asahara et al.³⁴ These elongated cells were early EPCs. The number of EPCs was reduced after 10 days (Figure S1A: e,f), and by day 28, they had gradually disappeared. In the meantime, cells displaying a cobblestone appearance and a smoother cytoplasmic outline similar to human umbilical vein endothelial cells appeared at 3 to 4 weeks of culture (Figure S1A: g,h). These cells were adherent, could uptake 1,1'-dioctadecyl-3,3',3'-tetramethylindo-carbocyanine-acetylated low-density lipoprotein, and could bind to FITC-lectin (Figure S1B). Flow cytometry showed that these cells expressed CD31 (endothelial marker), kinase-insert domain receptor (endothelial marker), and CD34 (stem cells

marker) but not CD133, CD14, and CD45 (leukocyte marker) (Figure S1C and Figure S2A). Therefore, late EPCs were successfully isolated, with characteristics previously described.^{31,32,35} The late cells showed capillary formation capacity (Figure S2B). The early cells showed higher levels of VEGF and interleukin-8 (Figure S2C and S2D), while stromal cell-derived factor 1 was not elevated (Figure S2E).

Effect of gCTRP9 on EPC Functions in Adhesion, Migration, and Vasculogenesis

The role of CTRP9 in EPC migration was examined. After 24 hours of incubation, the administration of gCTRP9 with increased concentrations (0.5–10 µg/mL) significantly enhanced EPC migration (0.5–10 µg/mL, all $P < 0.05$; Figure 1A). As shown in Figure 1B, EPC adhesion to fibronectin-coated dishes was enhanced in response to gCTRP9 treatment (30 minutes) in a concentration–response manner (0.5–10 µg/mL, all $P < 0.05$; Figure 1B).

The role of CTRP9 on EPC angiogenesis was investigated. EPCs were incubated with gCTRP9 0.5

to 10 µg/mL for 24 hours. As shown in Figure 1C, gCTRP9 led to an increased EPC tubule network on ECMatrix gel compared with the control group (all $P < 0.05$; Figure 1C). These results indicate that CTRP9 improved EPC functions by enhancing migration, adhesion, and vasculogenesis.

Effect of gCTRP9 on Akt, eNOS Activation, and Nitrite Production in EPCs

CTRP9 at physiological concentrations increases NO production by eNOS in endothelial cells.¹⁶ In addition, eNOS activity is pivotal to EPC functions and mobilization.^{36,37} Accordingly, we investigated gCTRP9 on Akt and eNOS activities in EPCs treated with gCTRP9 (0.5–10 µg/mL) for up to 2 hours in normal and HG conditions. As shown in Figure 2A and Figure S3A, the phosphorylation of eNOS (P-eNOS) at Ser¹¹⁷⁷ and Akt (P-Akt) at Ser⁴⁷³ displayed a concentration-dependent upregulation in EPCs after gCTRP9 treatment (increased P-eNOS, 2.5-fold; P-Akt, 2.2-fold by gCTRP9 5 µg/mL versus the control group; Figure 2A) (increased P-eNOS, 2.2-fold; P-Akt, 2.2-fold by gCTRP9

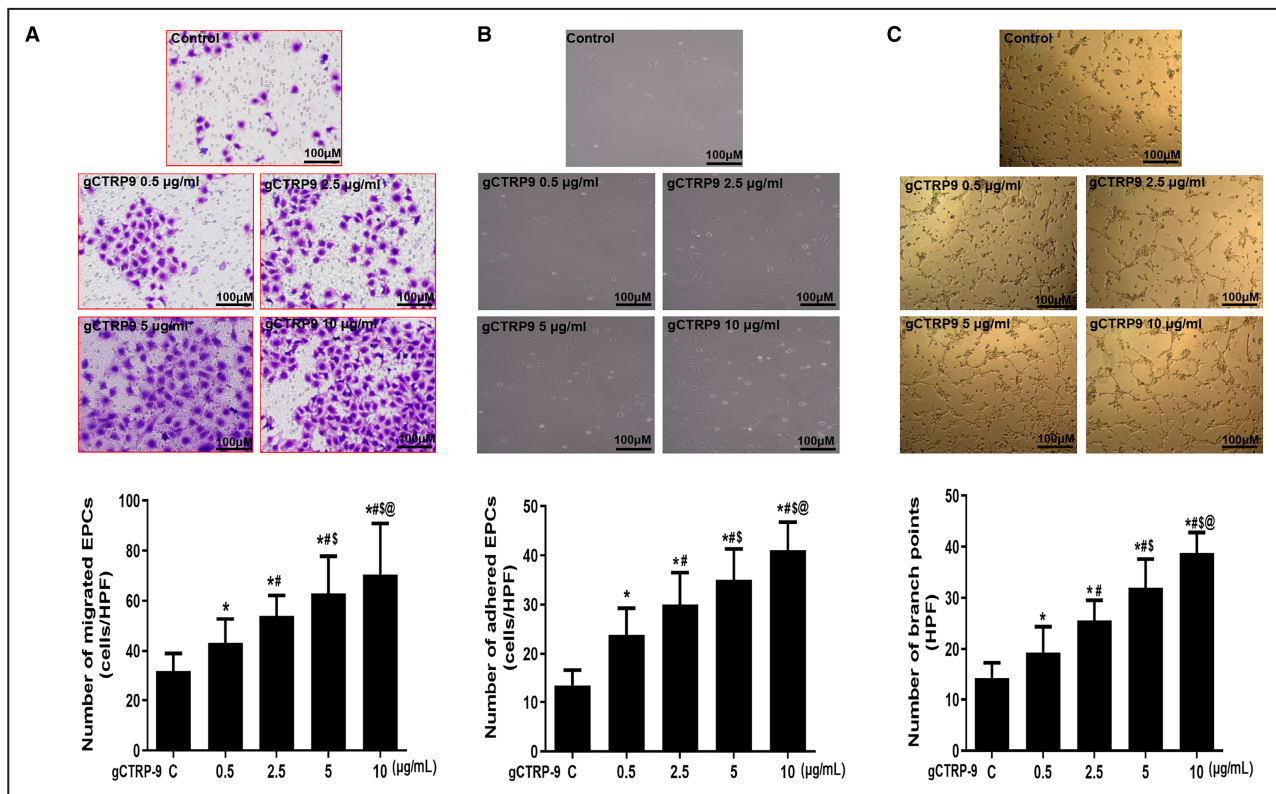


Figure 1. Effects of physiological levels of gCTRP9 on late EPC functions.

A, Cultured EPCs were incubated with gCTRP9. A Boyden chamber assay was performed to test the effect of gCTRP9 on migration. The migrated cells were stained with crystal violet and counted under a microscope (scale bar=100 µm). **B**, EPCs treated with gCTRP9 were harvested and plated on fibronectin-coated cell culture plates. The attached cells were photographed and quantified in high-power fields under an inverted microscope (scale bar=100 µm). **C**, EPCs were incubated with gCTRP9, and an in vitro angiogenesis assay was used to evaluate the effect of CTRP9 on EPC vasculogenesis (scale bar=100 µm). For all experiments, n=5, * $P < 0.05$ vs the control group, # $P < 0.05$ vs the 0.5 µg/mL gCTRP9 treatment group, \$ $P < 0.05$ vs the 2.5 µg/mL gCTRP9 treatment group, @ $P < 0.05$ vs the 5 µg/mL gCTRP9 treatment group. EPC indicates endothelial progenitor cell; gCTRP9, globular C1q/tumor necrosis factor-related protein-9; and HPF, high-power field.

5 µg/mL versus the HG group; [Figure S3A](#)). Increased eNOS and Akt phosphorylation was also noted after treatment with gCTRP9 for 24 hours in normal and HG condition (increased P-eNOS, 2.4-fold; P-Akt, 2.1-fold by gCTRP9 5 µg/mL versus the control group; [Figure 2B](#)) (increased P-eNOS, 2.4-fold; P-Akt, 2.1-fold by gCTRP9 5 µg/mL versus the HG group; [Figure S3B](#)). In addition, treatment with gCTRP9 (0.5–10 µg/mL) for 2 and 24 hours also concentration-dependently increased nitrite production by EPCs in the normal and HG conditions ([Figure 2C and 2D and Figure S3C and S3D](#), all $P < 0.01$). The eNOS phosphorylation levels were positively correlated with increased EPCs-derived nitrite production ([Figure 2E and 2F and Figure S3E and S3F](#), both $P < 0.01$). In addition, to rule out the effect of osmotic pressure, EPCs were treated with HG (25 mmol/L) or mannitol (25 mmol/L) for 4 days. HG markedly decreased eNOS expression, eNOS, Akt phosphorylation, and nitrite production. On the other hand, mannitol did not exert any influence on the above cell functions ($*P < 0.05$ versus the control or mannitol group; [Figure S4A through S4C](#)). These results indicate that gCTRP9 increased Akt and eNOS activation, leading to increased nitrite production in the normal and HG conditions (as a marker of NO production).

Effects of gCTRP9 on HG-Suppressed EPC Functions and HG-Induced Senescence

First, to rule out the effect of osmotic pressure, EPCs were treated with HG (25 mmol/L) or mannitol (25 mmol/L) for 4 days. HG significantly impaired the migration, adhesion, and tube formation of EPCs and increased cell senescence. On the other hand, mannitol did not exert any influence on the above in vitro functions ($*P < 0.05$ versus the control or mannitol group; [Figure S5A through S5D](#)). We then investigated whether the administration of gCTRP9 could improve HG-suppressed EPC functions. As previously shown,^{38,39} the incubation of EPCs in an HG medium (25 mmol/L) for 4 days attenuated the migratory capacity of the EPCs ($*P < 0.05$ versus the control group; [Figure 3A](#)). The administration of gCTRP9 for 24 hours followed by treatment of EPCs in the HG environment significantly enhanced HG-impaired EPCs migration ($P < 0.05$ versus the HG group; $P < 0.05$ versus the 2.5 µg/mL gCTRP9+HG group; $P < 0.05$ versus the 5 µg/mL gCTRP9+HG group; [Figure 3A](#)).

As shown in [Figure 3C](#), EPCs cultured in the HG environment for 4 days displayed markedly decreased tube formation capacity ($P < 0.05$ versus the control group). Treatment of gCTRP9 (5 µg/mL) for 24 hours followed by HG medium significantly improved the HG-suppressed tube formation capacity of EPCs ($P < 0.05$ versus the HG group; $P < 0.05$ versus the 2.5 µg/mL

gCTRP9+HG group; $P < 0.05$ versus the 5 µg/mL gCTRP9+HG group; [Figure 3C](#)).

EPC senescence was examined using acidic β-galactosidase. Compared with the control group, treatment of EPCs with HG medium for 4 days markedly increased the number of senescent β-galactosidase-positive cells ($P < 0.05$; [Figure 3B](#)). Administration of gCTRP9 (5 µg/mL) for 24 hours followed by treatment of EPCs under HG conditions reduced the number of senescent β-galactosidase-positive cells ($P < 0.05$ versus the HG group; [Figure 3B](#)). Treatment with L-NAME (an eNOS inhibitor, 100 µmol/L) decreased the antisenescence role of CTRP9 on EPCs in the HG environment ($P < 0.05$ versus the 5 µg/mL gCTRP9+HG group; [Figure 3B](#)).

As shown in [Figure 3D](#), incubation of EPCs with HG medium decreased EPC adhesion ($P < 0.05$ versus the control group). gCTRP9 (5 µg/mL) enhanced EPC adhesion under HG conditions (HG versus HG+gCTRP9 group; $P < 0.05$). This enhanced EPC adhesion was inhibited by L-NAME (100 µmol/L) (HG+gCTRP9+L-NAME treatment groups versus HG+gCTRP9 group; $P < 0.05$). In addition, treatment with the NO donor sodium nitroprusside (100 µmol/L) induced similar effects of gCTRP9 to improve HG-suppressed EPC adhesion (all sodium nitroprusside treatment groups versus HG group; $P < 0.05$). Because the sodium nitroprusside+gCTRP9 group was not better than sodium nitroprusside alone or HG+gCTRP9, and because L-NAME+HG was not significantly lower than L-NAME or HG, the results suggest that the phenotypic changes were not only caused by the effects of gCTRP9 on eNOS but that other pathways or regulatory mechanisms were also involved. Nevertheless, the findings suggest that the administration of gCTRP9 might restore impaired EPC functions under HG conditions, and these benefits might derive from NO-associated mechanisms.

gCTRP9 Restored HG-Impaired eNOS Activation and NO Production

HG attenuates eNOS activation and reduces NO bioavailability through posttranslational modification at the Akt site in cultured EPCs.³⁹ Therefore, we evaluated gCTRP9 on HG-treated EPCs to determine the ability of CTRP9 to restore the decreased eNOS activation in EPCs. After 4 days, the HG medium (25 mmol/L) significantly downregulated the phosphorylation of eNOS at Ser¹¹⁷⁷, Akt at Ser⁴⁷³, and total eNOS ([Figure 4A](#)), and it was associated with decreased EPC-derived NO production ([Figure 4B](#)). Meanwhile, the administration of gCTRP9 under HG conditions for 24 hours concentration-dependently upregulated the eNOS and Akt phosphorylation and total eNOS and increased NO production ([Figure 4A and 4B](#)).

To confirm the role of eNOS in the enhancement of HG-impaired EPC functions by CTRP9, EPCs were transfected with eNOS siRNA to inhibit eNOS activity. As shown in [Figure 4C](#), treatment with 25 and 50 nmol/L eNOS siRNA inhibited eNOS expression by administering gCTRP9 under HG conditions. Treatment with eNOS siRNA led to an inhibition of eNOS expression and markedly impaired the benefits of CTRP9 in improving EPC vasculogenesis ([Figure 4D](#)). Therefore, these results suggest that gCTRP9 restored HG-impaired eNOS activation and NO production.

Effects of AMPK in CTRP9-Modulated EPC Function and eNOS Activation

Previous studies showed that AMPK could cause direct or indirect eNOS phosphorylation through Akt activation and could be involved in CTRP9-mediated biological actions.^{16,40} Hence, it could be hypothesized that CTRP9 could act on AMPK in EPCs. After incubation of EPCs with gCTRP9 (2.5–10 μmol/L) for 2 hours in the normal and HG conditions, the phosphorylation levels of AMPK were analyzed. As shown in [Figure 5A](#) and [Figure S6A](#), EPCs cultured with gCTRP9 showed markedly increased phosphorylation of AMPK at the Thr¹⁷² site, and treatment with an AMPK inhibitor (Compound C, 10 μmol/L) for 30 minutes inhibited gCTRP9-upregulated AMPK, eNOS, and Akt phosphorylation ([Figure 5B](#) and [Figure S6B](#)). In addition, treatment with an Akt inhibitor (LY294002, 10 μmol/L) for 30 minutes did not exert an inhibitory effect on the phosphorylation of AMPK but blocked (although incompletely) CTRP9-induced Akt and eNOS phosphorylation ([Figure 5C](#) and [Figure S6C](#)). These results suggested that AMPK might act as an upstream signal element of Akt involved in CTRP9-induced eNOS phosphorylation and its derived positive biological effects.

We evaluated the role of AMPK in CTRP9-induced upregulation of Akt and eNOS activities under HG conditions. First, to rule out the effect of osmotic pressure, EPCs were treated with HG (25 mmol/L) or mannitol (25 mmol/L) for 4 days. HG significantly impaired the phosphorylation of AMPK but not mannitol ($P < 0.05$ versus the control or mannitol group; [Figure S4D](#)). EPCs were treated with an AMPK inhibitor (Compound C, 1 and 10 μmol/L) before gCTRP9 (5 μg/mL) for 24 hours under HG medium. As shown in [Figure 5D](#), the activation of the phosphorylation of Akt and eNOS

by gCTRP9 was impaired by Compound C under HG conditions. Moreover, the beneficial effect of CTRP9 on HG-suppressed EPC migration was markedly blocked by the treatment with an AMPK inhibitor (Compound C; [Figure 5E](#)), indicating that CTRP9 may enhance HG-impaired EPC function through the AMPK-mediated Akt/eNOS pathway.

AdipoR1, AdipoR2, and N-Cadherin in CTRP9-Mediated eNOS Activation and EPC Function

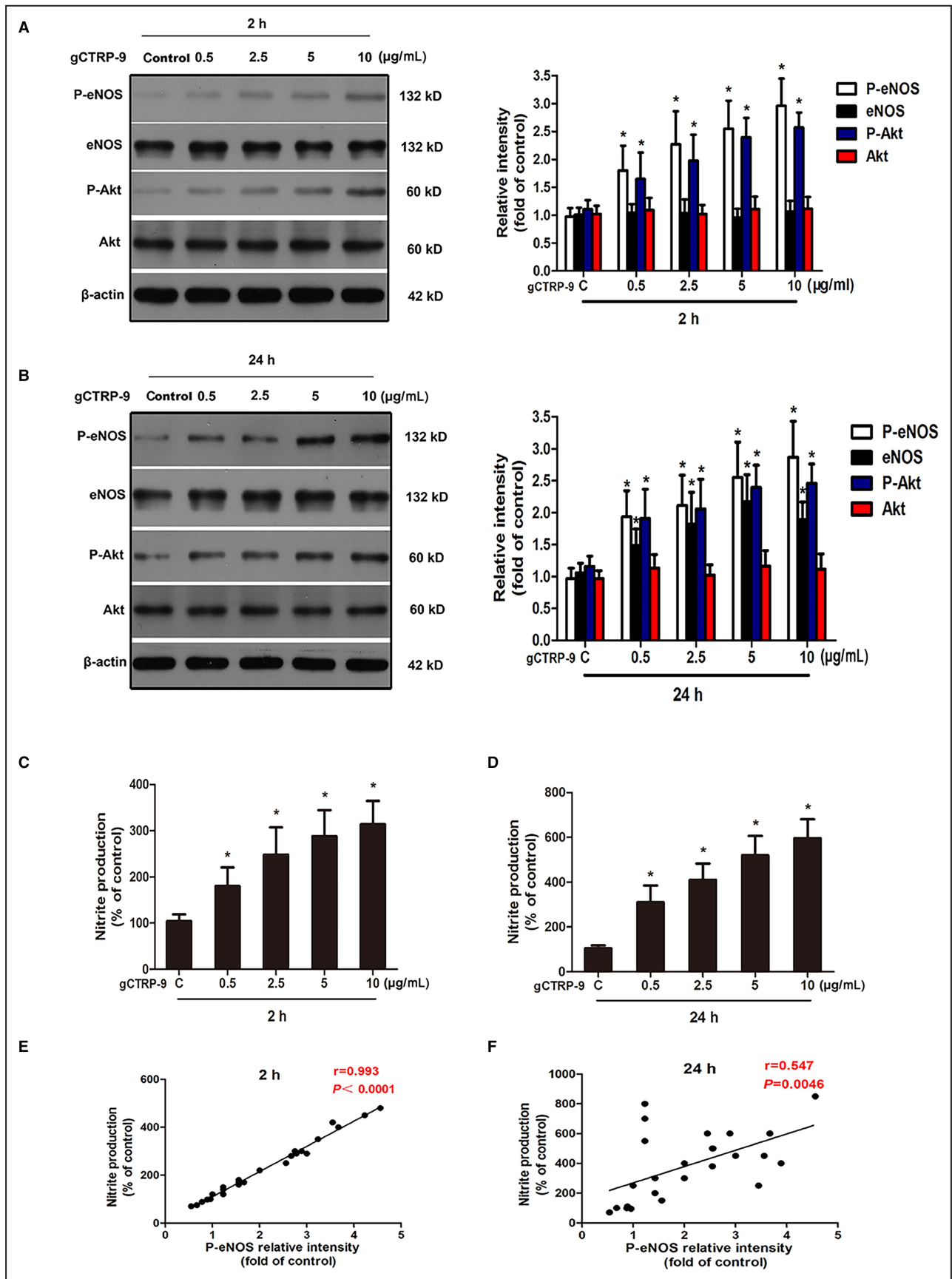
Two CTRP9 receptors, adipoR1 and adipoR2, could mediate CTRP9's collectin-like functions.¹⁶ In order to examine the involvement of adipoR1 and adipoR2 in CTRP9-mediated AMPK, eNOS activation, and EPC function under HG conditions, siRNAs were used to silence endogenous adipoR1 and adipoR2 expression. Then, after 48 hours, the EPCs were treated with vehicle or CTRP9 (5 μg/mL) for 24 hours. The siRNA-induced suppression of adipoR1 and adipoR2 was confirmed (each 75%–80%) ([Figure 6A](#) and [6B](#)). The administration of CTRP9 upregulated adipoR1 and adipoR2 expression, while HG stimulation impaired adipoR1 and adipoR2 expression. In addition, treatment with gCTRP9 restored adipoR1 and adipoR2 expression after HG stimulation ([Figure 6A](#) and [6B](#)). These results suggested that adipoR1 and adipoR2 mediated CTRP9-induced cytoprotective effects in an HG environment.

As shown in [Figure 6C](#) and [6G](#), the silencing of adipoR1, but not adipoR2, reduced gCTRP9-induced phosphorylation of AMPK, Akt, and eNOS after treatment with gCTRP9 under HG conditions. No significant differences were observed in these outcome parameters between adipoR2 knockdown and scrambled siRNA-treated cells. Moreover, the administration of adipoR1 siRNA (50 nmol/L) impaired EPC migration under HG conditions ([Figure 6H](#)). These findings indicated that gCTRP9 induced AMPK/Akt/eNOS pathway activation.

It should be worth paying attention to a recent study suggesting that N-cadherin is a novel CTRP9 receptor of adipose-derived mesenchymal stem cells involved in protective effects against ischemic heart injury.⁴⁰ Hence, it could be hypothesized that N-cadherin could also be a potential receptor for CTRP9 on EPCs. As illustrated in [Figure S7A](#), immunocytochemistry demonstrated the colocalization of CD31 and N-cadherin on

Figure 2. Effects of gCTRP9 on eNOS, Akt, and NO production in EPCs in the normal condition.

A and **B**, Effects of gCTRP9 on eNOS, Akt activities, and nitrite levels were determined in late EPCs. Administration of gCTRP9 (2 and 24 hours) concentration-dependently increased phosphorylation of eNOS (P-eNOS) and Akt (P-Akt). **C** and **D**, Nitrite production (as NO content) in culture medium was measured by Griess reagent. **E** and **F**, Correlation of P-eNOS relative intensity with nitrite production in EPCs. Correlations between P-eNOS relative intensity and the variables were performed using Spearman correlation analysis. For all experiments, $n=5$, $*P < 0.01$ vs the control group. Akt indicates protein kinase B; eNOS, endothelial nitric oxide synthase; EPC, endothelial progenitor cell; gCTRP9, globular C1q/tumor necrosis factor-related protein-9; NO, nitric oxide; and P-, phosphorylated.



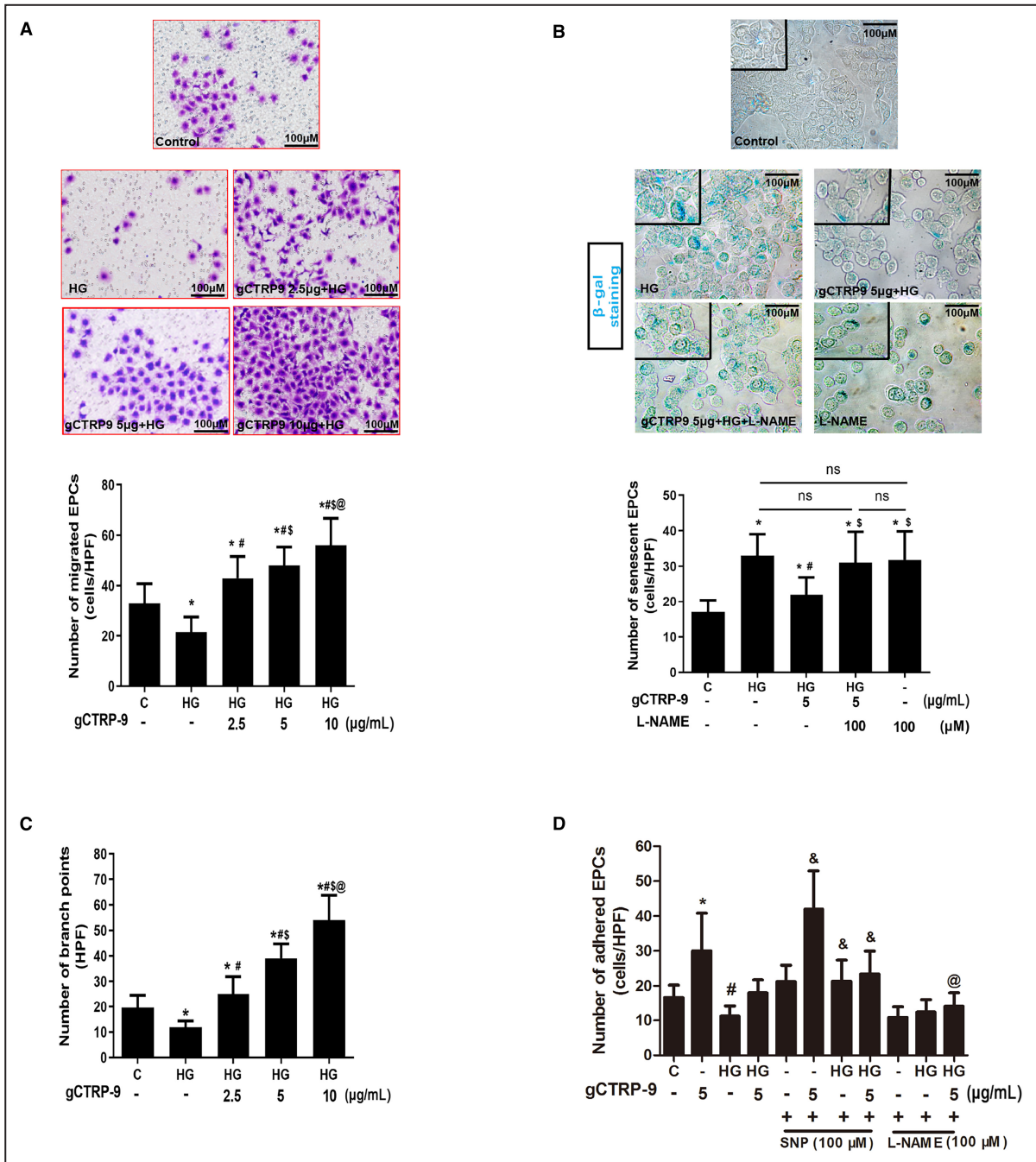


Figure 3. CTRP9 recovered HG-impaired EPC functions and attenuated cellular senescence.

After incubating EPCs with the indicated concentrations of gCTRP9 for 24 hours, the EPCs were evaluated using functional experiments after treatment with HG for 4 days. **A**, A modified Boyden chamber assay was used to evaluate the effect of gCTRP9 on migration (scale bar=100μm) (n=5), *P<0.05 vs the control group, #P<0.05 vs the HG group, \$P<0.05 vs the 2.5μg/mL gCTRP9+HG group, @P<0.05 vs the 5μg/mL gCTRP9+HG group. **B**, β-galactosidase was detected as a marker for acidification typical of cell senescence (scale bar=100μm) (n=5), *P<0.05 vs the control group, #P<0.05 vs the HG group, \$P<0.05 vs the 5μg/mL gCTRP9+HG group. **C**, An in vitro angiogenesis assay was performed with EPCs to investigate the role of gCTRP9 on EPC vasculogenesis under HG conditions (n=5), *P<0.05 vs the control group, #P<0.05 vs the HG group, \$P<0.05 vs the 2.5μg/mL gCTRP9+HG group, @P<0.05 vs the 5μg/mL gCTRP9+HG group. **D**, The fibronectin adhesion assay was used to evaluate the effect of gCTRP9 on EPCs adhesive capacity (n=5), *P<0.05 vs the control group, #P<0.05 vs the HG group, &P<0.05 vs the HG+gCTRP9 group, @P<0.05 vs the HG+gCTRP9 group. Akt indicates protein kinase B; eNOS, endothelial nitric oxide synthase; EPC, endothelial progenitor cell; gCTRP9, globular C1q/tumor necrosis factor-related protein-9; HG, high glucose; L-NAME, N(ω)-nitro-L-arginine methyl ester; and NO, nitric oxide.

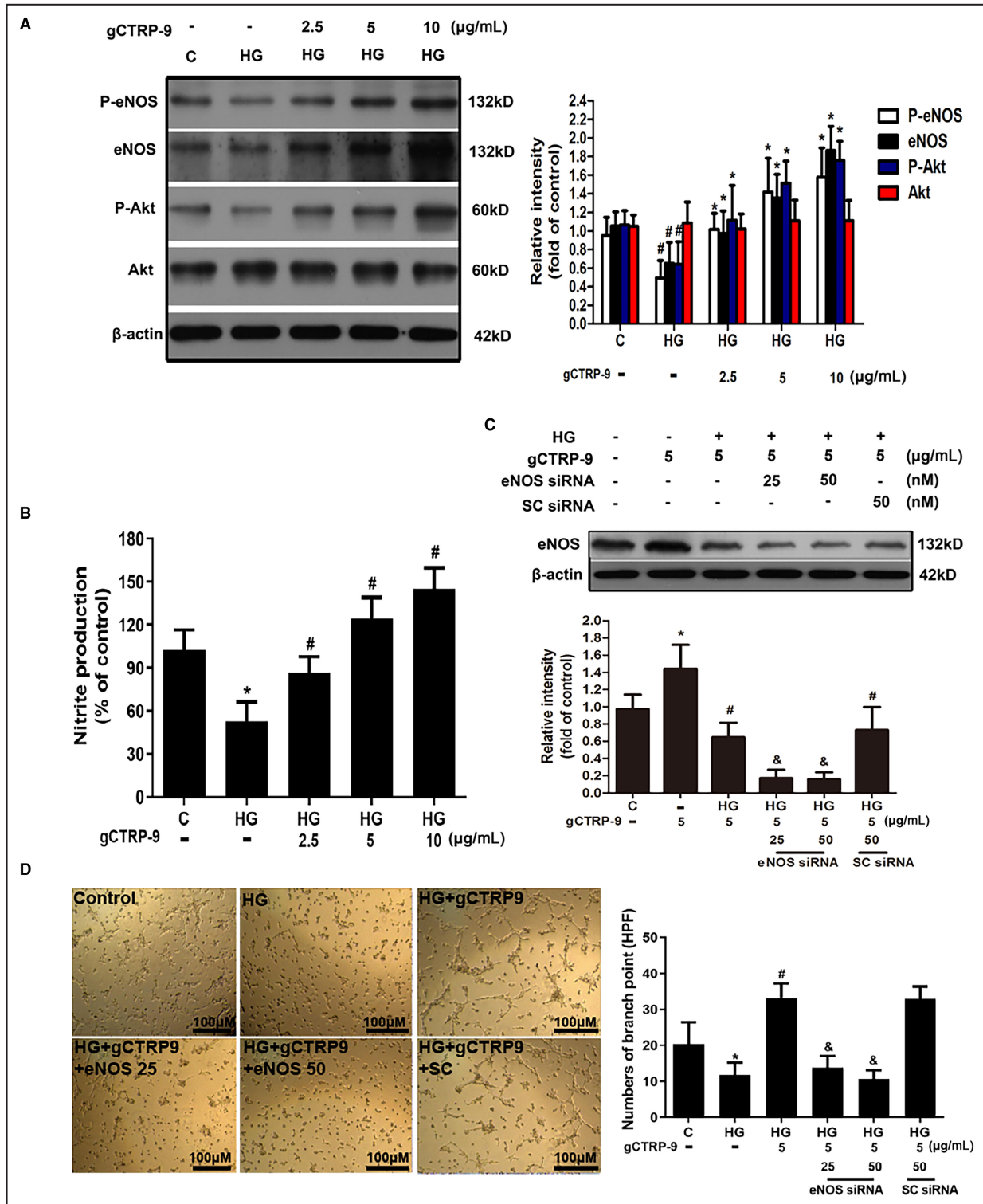


Figure 4. CTRP9 recovered HG-impaired EPC activation and NO production.

A, Effects of gCTRP9 on total eNOS and Akt. eNOS and Akt phosphorylation was determined in EPCs. **B**, Nitrite production (as NO content) in culture medium was measured by Griess reagent. (For **A** and **B**, n=5, *P<0.05 vs the control group, #P<0.05 vs the HG group). **C**, Treatment using eNOS siRNA (25 and 50 nmol/L) decreased the accumulation of eNOS by administration of gCTRP9 under HG medium. **D**, An in vitro angiogenesis was used to investigate the effect of gCTRP9 on EPCs vasculogenesis under HG medium after knockdown of eNOS activity (scale bar=100 μ m). (For **C** and **D**, n=5, *P<0.05 vs the control group, #P<0.05 vs the HG group, &P<0.05 vs the HG+gCTRP9 group). Akt indicates protein kinase B; eNOS, endothelial nitric oxide synthase; EPC, endothelial progenitor cell; gCTRP9, globular C1q/tumor necrosis factor-related protein-9; HG, high glucose; NO, nitric oxide; P, phosphorylated; and siRNA, small inhibitory RNA.

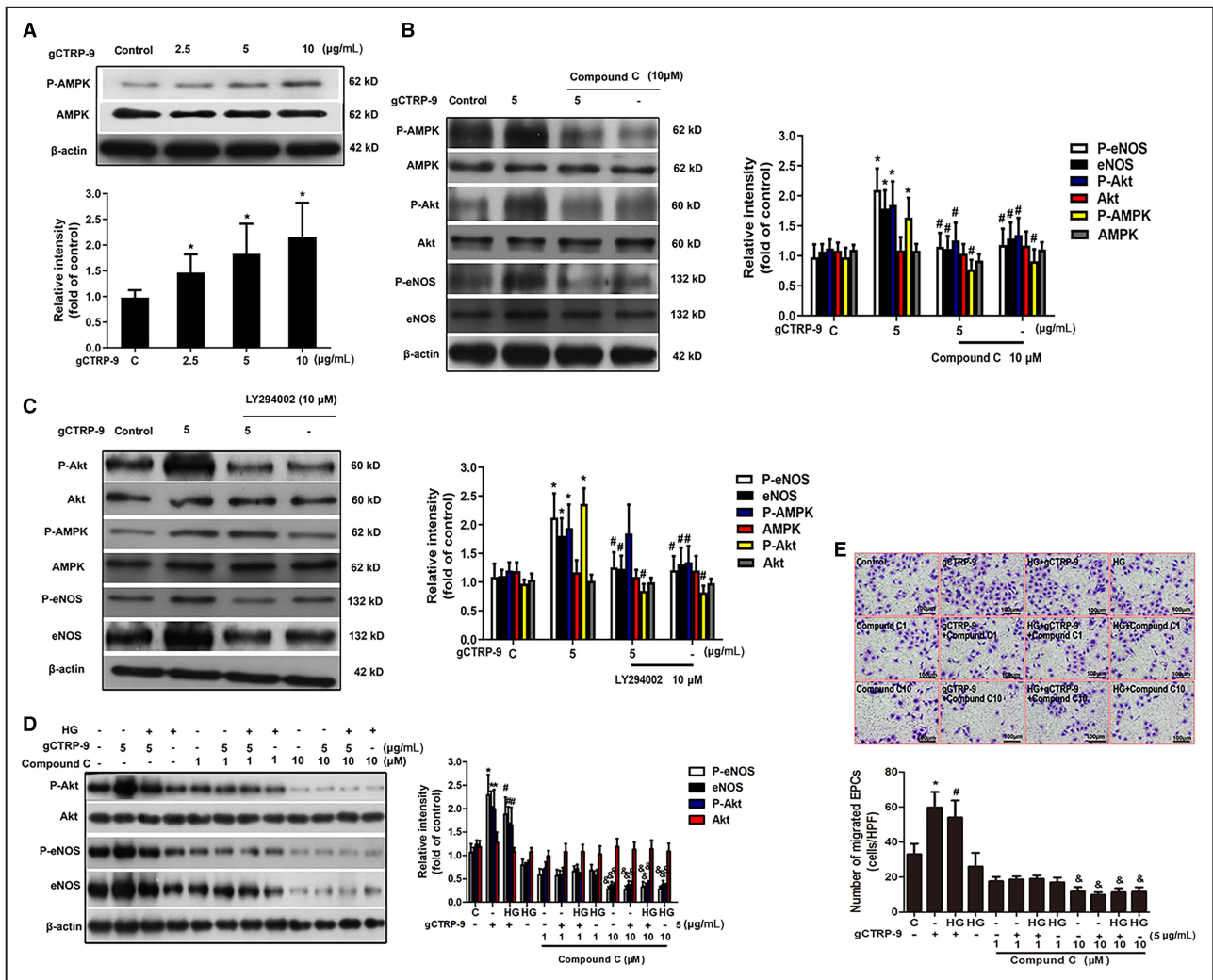


Figure 5. Effects of AMPK in CTRP9-modulated EPC function and eNOS activation.

A, After incubation of EPCs with the indicated concentrations of gCTRP9 for 2 hours, AMPK protein phosphorylation and total protein levels were analyzed. **B**, EPCs were incubated with an AMPK inhibitor (Compound C, 10 µmol/L) for 30 minutes, followed by gCTRP9 (5 µg/mL) for 24 hours. Phosphorylated and total eNOS, Akt, and AMPK were measured. **C**, EPC incubation with Akt inhibitor (LY294002, 10 µmol/L) for 30 minutes, followed by gCTRP9 (5 µg/mL) for 24 hours. eNOS, Akt, and AMPK (phosphorylated and total forms) were measured. **D**, Effects of CTRP9 on eNOS and Akt (phosphorylated and total forms) in EPCs after pretreatment with Compound C under HG conditions. **E**, A Boyden chamber test was performed to evaluate the effect of CTRP9 on EPC migration (scale bar=100 µm). For all experiments, n=5, *P<0.05 vs the control group, #P<0.05 vs the 1-µM Compound C group. Akt indicates protein kinase B; AMPK, AMP-activated protein kinase; eNOS, endothelial nitric oxide synthase; EPC, endothelial progenitor cell; gCTRP9, globular C1q/tumor necrosis factor-related protein-9; HG, high glucose; NO, nitric oxide; and P-, phosphorylated.

the EPC membrane, suggesting that EPCs expressed N-cadherin protein. To evaluate whether N-cadherin was involved in CTRP9-mediated AMPK, eNOS activation, and EPC function under HG conditions, we also used siRNA to downregulate N-cadherin expression. N-cadherin was knocked down using the same system as adipoR1 and adipoR2. The Western blotting analysis confirmed a siRNA-induced suppression of 80%. Similar to adipoR1 and adipoR2, treatment with gCTRP9 upregulated N-cadherin expression, while HG impaired N-cadherin expression. Moreover, treatment with gCTRP9 restored N-cadherin expression

after HG stimulation (Figure S7B). N-cadherin siRNA markedly decreased the activation of AMPK, Akt, and eNOS phosphorylation (Figure S7C through S7F) and attenuated EPC migratory capacity by treatment with gCTRP9 in the HG environment (Figure S7G). In addition, to rule out the effect of osmotic pressure, EPCs were treated with HG (25 mmol/L) or mannitol (25 mmol/L) for 4 days. HG significantly impaired the expression of adipoR1 and N-cadherin but not mannitol (P<0.05 versus the control group or the mannitol group; Figure S4E through S4G). The results revealed that CTRP9 restored HG-induced impaired EPC

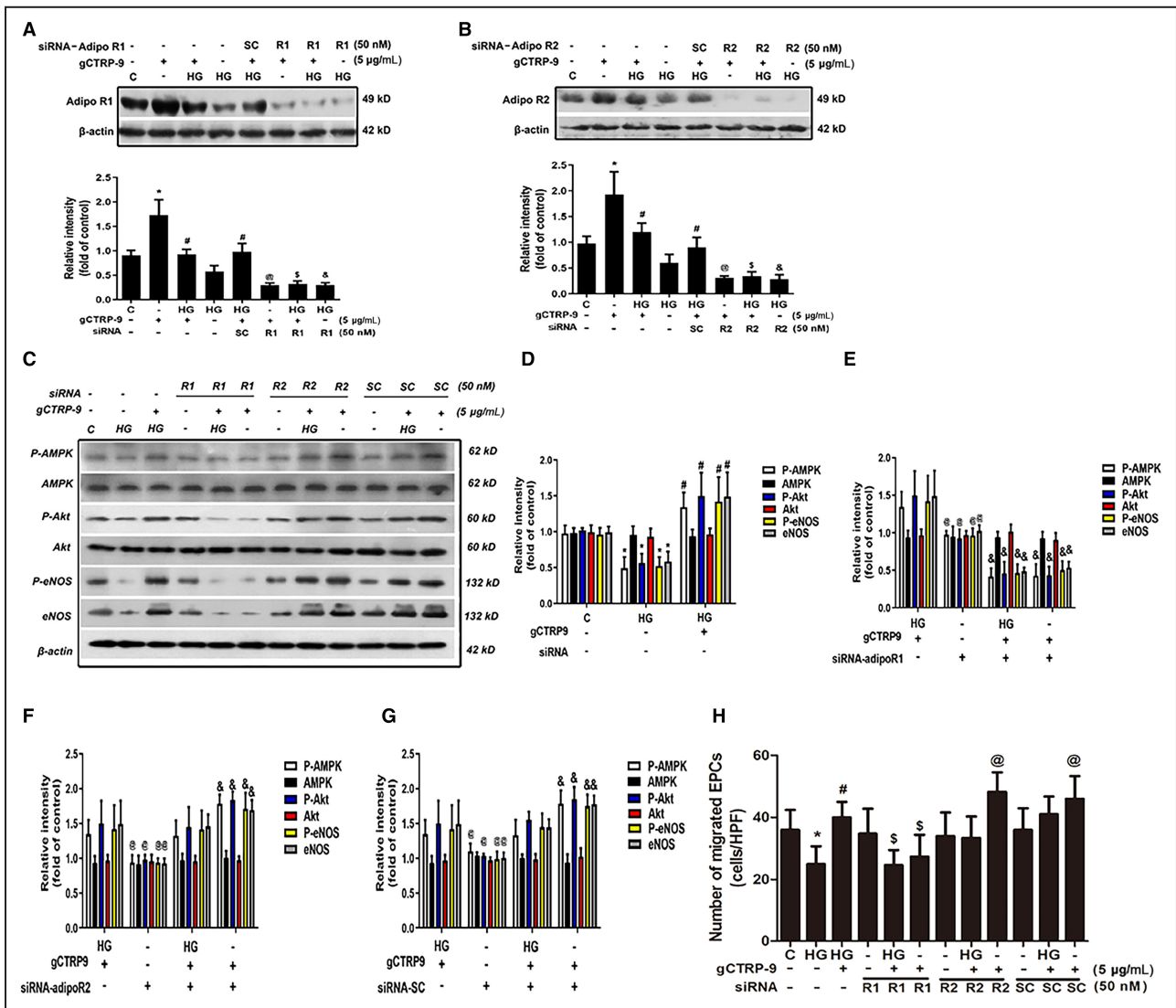


Figure 6. Effect of adipoR1 and adipoR2 in CTRP9-upregulated eNOS activation and EPC function. **A** and **B**, Treatment with gCTRP9 upregulated adipoR1 and adipoR2 expression. HG stimulation impaired adipoR1 and adipoR2 expression. Administration of CTRP9 restored adipoR1 and adipoR2 expression under HG conditions. Administration of adipoR1 siRNA (50nmol/L) or adipoR2 siRNA (50nmol/L) knocked down adipoR1 and adipoR2 protein expression under CTRP9 and HG treatment (n=5), *P<0.05 vs the control group, #P<0.05 vs the HG group, @P<0.05 vs the gCTRP9 treatment group, \$P<0.05 vs the gCTRP9+HG group, &P<0.05 vs the HG group. **C** through **G**, The administration of adipoR1 siRNA (50nmol/L) significantly attenuated the activation of eNOS, Akt, and AMPK by treatment with gCTRP9 under HG conditions. **H**, The administration of adipoR1 siRNA (50nmol/L) impaired EPC migration under HG conditions. For **C** through **H**, n=5, *P<0.05 vs the control group, #P<0.05 vs the HG group, @P<0.05 vs the gCTRP9+HG group, \$P<0.05 vs the siRNA (adipoR1, adipoR2, and scrambled siRNA) treatment group. adipoR1 indicates adiponectin receptor 1; adipoR2, adiponectin receptor 2; Akt, protein kinase B; AMPK, AMP-activated protein kinase; eNOS, endothelial nitric oxide synthase; EPC, endothelial progenitor cell; gCTRP9, globular C1q/tumor necrosis factor-related protein-9; HG, high-glucose; NO, nitric oxide; and siRNA, small inhibitory RNA.

functions through adipoR1 and N-cadherin-mediated eNOS activation.

gCTRP9-Treated EPC Transplantation Improved In Vivo Reendothelialization After Arterial Injury

We first investigated whether the carotid artery expressed the receptors for CTRP9. AdipoR1- and adipoR2-positive cells (red and green staining in

Figure 7A and 7B, respectively) were localized on the lumen surfaces in normal carotid arteries, indicating that these cells were also endothelial-positive cells. To confirm this, the colocalization studies using anti-CD31 and anti-α-SMA antibodies revealed that CD31+ cells in the lumens of arteries coexpressed adipoR1 and adipoR2 on the endothelium layer, whereas α-SMA+ cells did not express these proteins (Figure 7A and 7B). N-cadherin-positive cells (red staining in Figure S7H) were observed in the middle and lumen surface in normal carotid

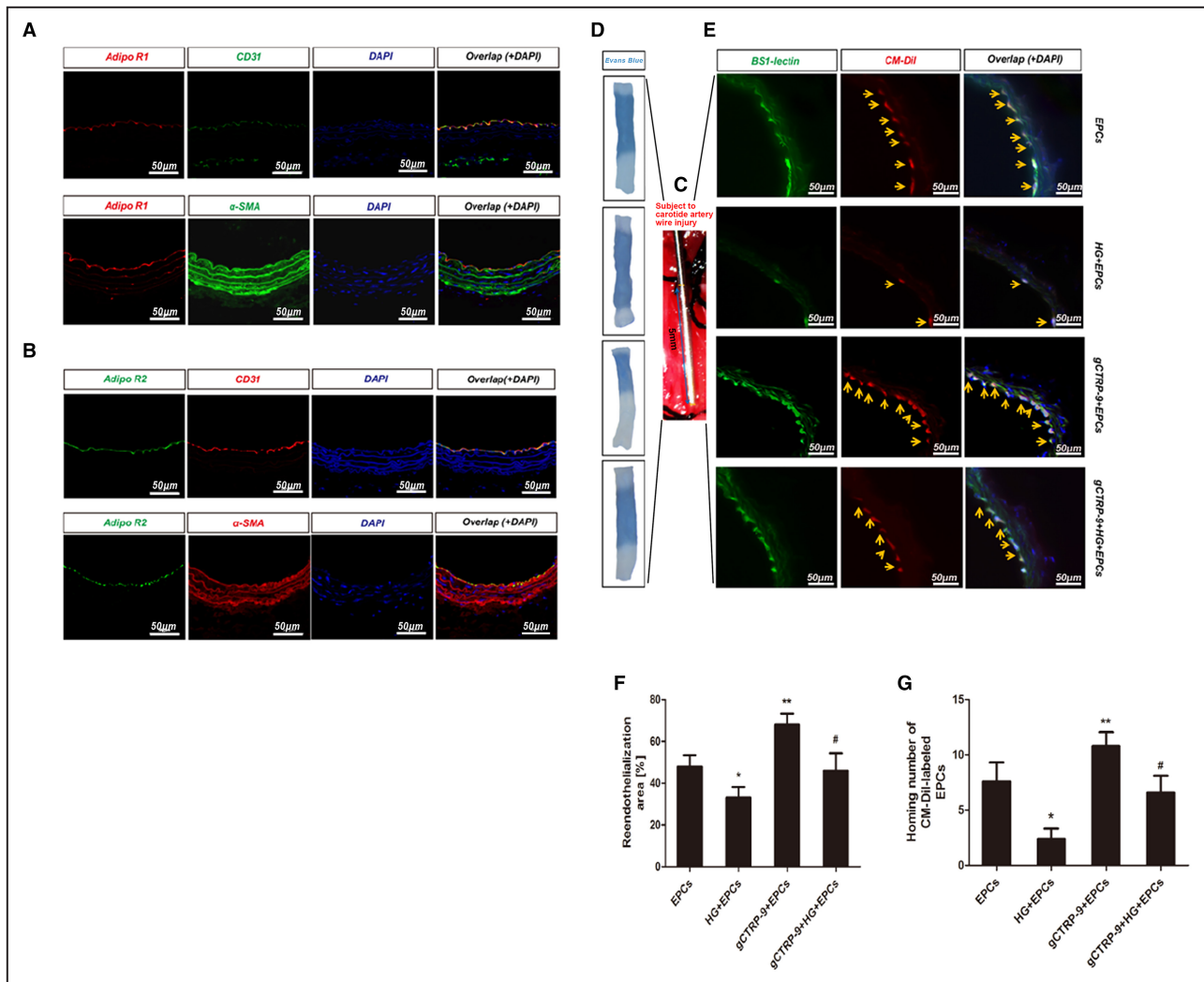


Figure 7. CTRP9-treated EPC transplantation promoted reendothelialization after vascular injury in mice.

A, Double-immunofluorescence images for adipoR1 (red) and CD31 (green), or α -SMA (green), showed coexpression of adipoR1 in CD31⁺ cells. (Scale bar=50 μ m). **B**, Double-immunofluorescence images for adipoR2 (green) and CD31 (red), or α -SMA (red), showed coexpression of adipoR2 in CD31⁺ cells (scale bar=50 μ m). **C**, Nude mice were subjected to the carotid artery injury model. **D** through **F**, Evans blue dye was injected 10 minutes before euthanasia on day 5. Nonendothelialized lesions were marked by blue staining, whereas the reendothelialized area appeared white. **E** through **G**, CM-Dil labeled EPCs (red) were transfused to nude mice after carotid artery injury on day 5. The localization of double-fluorescent cells, FITC-lectin/CM-Dil cells, was shown as yellow dots in the merged image. For all experiments, scale bar=50 μ m, n=5, * P <0.05 vs the EPC group, # P <0.05 vs the HG group, ** P <0.01 vs the EPC group. Akt indicates protein kinase B; eNOS, endothelial nitric oxide synthase; EPC, endothelial progenitor cell; gCTRP9, globular C1q/tumor necrosis factor-related protein-9; and HG, high-glucose.

arteries, as evidenced by the colocalization studies of CD31 and α -SMA.

Finally, we evaluated whether gCTRP9 could improve the in vivo reendothelialization capacity of HG-induced decline of EPC functions. A mouse carotid artery injury model was established to evaluate the in vivo reendothelialization capacity. Male nude mice were randomized to 4 treatment groups for intravenous transfusion of healthy EPCs, gCTRP9+EPCs, HG+EPCs, and HG+gCTRP9+EPCs (Figure 7C). Compared with the mice treated with HG+EPCs, the reendothelialization area (white area) of the healthy EPCs group was increased after vascular injury on

day 5 (33 \pm 3.5% versus 48 \pm 2.8%; P <0.05; Figure 7D and 7F). Injection of gCTRP9+EPCs could increase the regenerative endothelium area compared with the healthy EPCs group (68 \pm 3.3% versus 48 \pm 2.8%; P <0.05). Moreover, the reendothelialization area of the HG+gCTRP9+EPCs group was very similar to the healthy EPCs group. Confocal laser scanning microscopy showed that CTRP9 promoted transplanted CM-Dil-labeled EPCs to attach at the sites in the endothelial repair zone of the injured carotid artery (Figure 7E and 7G), suggesting that CTRP9 could enhance the effect of EPCs-mediated vascular repair under HG conditions.

DISCUSSION

The mechanisms underlying the vasculoprotective functions of CTRP9 remain unclear. This study aimed to investigate whether gCTRP9 could restore EPC functions that had been suppressed by HG through eNOS activation. The results suggest that physiological levels of gCTRP9 increased migration, adhesion, and tube formation in EPCs. Moreover, gCTRP9 up-regulated P-AMPK, P-Akt, and P-eNOS and increased nitrite production in a concentration-dependent manner. Exposure to HG induced EPC senescence and decreased eNOS activation and nitrite production. However, these detrimental effects were reversed by gCTRP9, which acts through adipor1 and N-cadherin-mediated AMPK/Akt/eNOS signaling. Nude mice injected with EPCs treated with CTRP9 under HG medium exhibited significantly enhanced reendothelialization capacity compared with those treated with EPCs incubated under HG conditions. Therefore, modulation of CTRP9 may improve the healing of vascular injuries.

Previous studies have suggested that circulating EPCs play a vital role in reendothelialization and neovascularization at the sites of endothelial injury or ischemia.^{4-8,21,41,42} Furthermore, decreased circulating EPCs independently predicted atherosclerosis progression and future acute vascular events.⁴³ Reduced numbers and impaired functions of EPCs in patients with type 2 diabetes have been attributed to diabetic vascular complications. Thus, EPCs hold therapeutic potential for vascular protection in such patients. The 2 types of EPCs, namely, early and late EPCs, exhibited functional differences *in vitro*. Early EPCs were unable to form tubelike structures, while late EPCs demonstrated a certain capacity for capillary formation. In contrast, early EPCs exhibited a stronger ability to secrete angiogenic factors compared with late EPCs. The concentration of well-known angiogenic cytokines, such as VEGF and interleukin-8, was significantly higher in the supernatant of early EPCs compared with that of late EPCs. Stromal cell-derived factor 1 levels did not show an increase in either of the supernatants. These findings align with the study conducted by Hur et al.³⁵ Consistent with previous research, this study found that human late EPCs' functions, namely, migration, adhesion, and vasculogenesis, were attenuated by HG. However, gCTRP9 could directly enhance EPC functions without HG or the dysfunctions caused by HG. These results support the role of CTRP9 in vascular protection, as proposed in previous studies.¹⁵⁻¹⁸ Indeed, exogenous gCTRP9 administration at physiological levels was found to improve endothelium-dependent vasodilation and enhance endothelial cell growth.¹⁶ Additionally, gene transfer of CTRP9 significantly inhibited vascular smooth muscle

cell proliferation and reduced neointima formation after vascular injury.¹⁷ Reduced plasma CTRP9 levels have been observed in type 2 diabetes¹⁹ and coronary artery disease patients.²⁰ Therefore, low CTRP9 levels might be a biomarker for predicting endothelial dysfunction and coronary plaque vulnerability. Although the mechanisms are unclear, CTRP9-knockout hearts showed negligible mesenchymal stem cell mobilization, which was restored by gCTRP9 administration.⁴⁰ Thus, the observed improvements in EPC functions after gCTRP9 treatment in this study are consistent with previous research on CTRP9.

HG impairs eNOS expression or its Ser1177 phosphorylation, leading to reduced bioavailability of NO, decreased proliferation, and increased apoptosis of endothelial cells, which may contribute to the development of atherosclerosis in diabetes.^{44,45} CTRP9 can increase NO production in endothelial cells by promoting the phosphorylation of eNOS at Ser1177 by Akt,^{16,39} indicating that increasing vascular NO bioavailability using CTRP9 might have vasoprotective effects at the endothelium level. In addition, eNOS expression and phosphorylation are essential for the survival, angiogenesis, and mobilization of EPCs.^{5-7,36,46} A recent study demonstrated that promoting eNOS phosphorylation could restore HG-induced impairment of EPCs.¹² Therefore, increasing EPCs and their functional capacities by enhancing eNOS-derived NO bioavailability using drugs could benefit patients with type 2 diabetes. In the present study, gCTRP9 enhanced Akt/eNOS phosphorylation and NO production, resulting in improved tube formation and migration capabilities of EPCs. This is supported by a previous study showing that CTRP9 stimulates the phosphorylation of Akt and eNOS in endothelial cells.¹⁶ Additionally, AMPK stimulates eNOS phosphorylation at Ser1177.⁴⁷ In the present study, EPCs treated with gCTRP9 displayed increased phosphorylation of AMPK at Thr172. To examine the hierarchy of AMPK and Akt signaling in CTRP9-induced eNOS phosphorylation, pharmacological inhibition of AMPK and Akt phosphorylation levels were performed in EPCs. The downregulation of the phosphorylation of either AMPK or Akt led to the significant attenuation of CTRP9-induced eNOS phosphorylation, suggesting that both AMPK and Akt are involved. After AMPK inhibition, CTRP9-induced Akt phosphorylation at Ser473 was blocked. On the other hand, Akt inhibition had no effect on CTRP9-induced AMPK Thr172 phosphorylation, suggesting that AMPK might be the most upstream molecule in CTRP9-induced eNOS phosphorylation. Moreover, the beneficial effects of CTRP9 on HG-impaired EPC migration were blocked by treatment with an AMPK inhibitor (Compound C). Therefore, CTRP9 could increase eNOS activation through the AMPK-mediated Akt/eNOS pathway.

CTRP9 acts through adipoR1 and adipoR2, which are surface membrane proteins that share a similar structure and are expressed in skeletal muscle, liver, and endothelial lineage cells.^{16,48–50} Before this study, it was completely unknown whether CTRP9 interacts with 1, both, or neither receptor in EPC. In this study, adipoR1 siRNA decreased the activation of AMPK, Akt, and eNOS and impaired EPC functions under treatment with gCTRP9 under HG conditions, while knocking down adipoR2 resulted in no significant effects. Notably, Yan et al⁴⁰ identified N-cadherin as a novel CTRP9 receptor in adipose-derived mesenchymal stem cells, and N-cadherin-mediated signaling protected cardiomyocytes against oxidative stress-induced cell death. Similarly, the immunohistochemistry results also showed that EPCs expressed N-cadherin. The administration of N-cadherin siRNA also decreased the activation of AMPK, Akt, and eNOS and impaired EPC functions under treatment with gCTRP9 and HG, suggesting that gCTRP9 promotes HG-suppressed EPC function via both adipoR1 and N-cadherin. Thus,

this study provided a novel mechanism for CTRP9 in vascular protection by improving late EPC function (Figure 8).

Moreover, this study indicated that EPCs treated with gCTRP9 could home to areas of vascular damage and participate in repairing the damaged endothelium in nude mice. HG-treated EPCs showed decreased homing and repair capacity, which was restored by gCTRP9 treatment. As EPCs play a major role in repairing endothelial damage,^{4–7} the results strongly suggest that gCTRP9 could eventually be used to restore EPC repair capacity in patients with type 2 diabetes or that EPCs from a patient could be boosted ex vivo using gCTRP9 and then re injected in the patient to increase repair after a vascular event. However, additional studies are necessary before any clinical application of gCTRP9.

This study possesses certain limitations that should be acknowledged. First, while we identified 2 receptors, adipoR1 and N-cadherin, involved in the CTRP9-induced vascular protective effects of EPCs in an HG

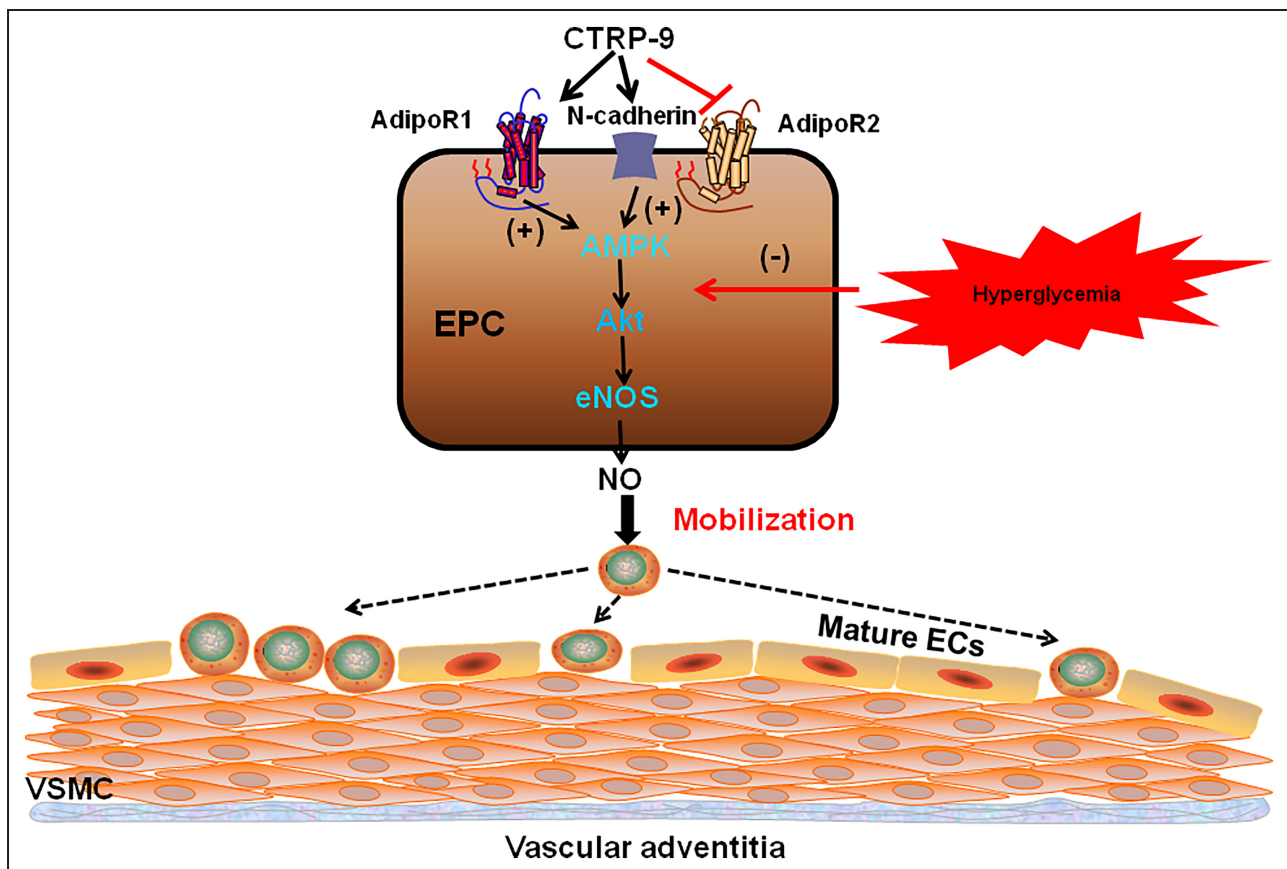


Figure 8. Schematic illustration of the pivotal role of CTRP9 in reendothelialization of EPCs and the protective mechanisms of AMPK-mediated Akt/eNOS signaling involved in adipoR1 and N-cadherin receptor.

Chronic exposure to HG impairs the reendothelialization capacity of EPCs. Treatment with gCTRP9 restores EPC functions and reendothelialization capacity under the HG environment through adipoR1 (not adipoR2) and N-cadherin-mediated AMPK/Akt/eNOS pathway. adipoR1 indicates adiponectin receptor 1; adipoR2, adiponectin receptor 2; Akt, protein kinase B; AMPK, AMP-activated protein kinase; EC, endothelial cell; eNOS, endothelial nitric oxide synthase; EPC, endothelial progenitor cell; gCTRP9, globular C1q/tumor necrosis factor-related protein-9; HG, high-glucose; and VSMC, vascular smooth muscle cell.

environment, further research is needed to determine the relative importance of each receptor-mediated signaling pathway. Second, due to experimental constraints, we were unable to use adipoR1, N-cadherin-specific endothelium conditional knockout models, or type 2 diabetes mice to assess the in vivo endothelial repair capacity of EPCs. Third, owing to experimental constraints, we only investigated an extreme glucose level of 25 mmol/L, and we were unable to examine the entire spectrum of diabetes. Nevertheless, such a high concentration of glucose may pose a risk of osmotic stress on the cells. The osmotic control (25 mmol/L mannitol) suggested that the observed changes in this study were not attributable to osmotic pressure, as previously observed in EPCs,³⁸ but in contradiction with 2 previous studies in human aortic endothelial cells.^{51,52} The discrepancy could be due to the nature of the cells; that is, EPCs are circulating cells that can adhere to injury sites and participate in new vessel formation,⁵³ while human aortic endothelial cells are fully differentiated cells found in the aortic vessel wall.⁵⁴ Nevertheless, the present study did not include human aortic endothelial cells, and future studies could examine that issue in several cell types in parallel. Finally, this study was primarily designed to investigate whether the administration of gCTRP9 could restore EPC functions suppressed by HG by activating eNOS. Therefore, the mechanisms explored were only preliminary, and additional studies will be necessary to elucidate the precise underlying mechanisms. This could involve comparisons with known agonists of EPC function, such as VEGF.

CONCLUSIONS

CTRP9 promotes EPC migration, adhesion, and tube formation and restores these functions under HG conditions through eNOS-mediated signaling mechanisms. These findings suggest that CTRP9 may serve as an endothelium regeneration agent that can enhance EPC functions both in vitro and in vivo. The use of CTRP9 and EPCs may have implications for the future management of patients with vascular diseases, particularly those with type 2 diabetes.

ARTICLE INFORMATION

Received March 3, 2023; accepted January 10, 2024.

Affiliations

Department of Cardiology (Q.H., T.Z., J.F., X.D.) and Health Management Center (W.Q.), First Affiliated Hospital of Jinan University, Guangzhou, China; Department of Cardiology, Guangdong Province Key Laboratory of Arrhythmia and Electrophysiology, Sun Yat-Sen Memorial Hospital of Sun Yat-Sen University, Guangzhou, China (R.N.); and Department of Cardiology, Fuwai Hospital, Chinese Academy of Medical Sciences (Shenzhen Sun Yat-Sen Cardiovascular Hospital), Shenzhen, China (J.C., X.W., C.P., X.K.).

Sources of Funding

This study was supported by grants from the National Natural Science Foundation of China (No. 82100348), the Guangdong Basic and Applied Basic Research Foundation of China (No. 2021A1515010178 and 2020A1515110865), the Science and Technology Projects in Guangzhou City, China (No. 202102021124), the Medical Science Technology Research Foundation of Guangdong Province of China (No. B2021162), the Fund of "Sanming" Project of Medicine in Shenzhen (SZSM201911017), and Shenzhen Fundamental Research Program, China (No. JCYJ20220531091611026).

Disclosures

None.

Supplemental Material

Figures S1–S7

REFERENCES

- Nathan DM, Cleary PA, Backlund JY, Genuth SM, Lachin JM, Orchard TJ, Raskin P, Zinman B, Diabetes C; Complications Trial/Epidemiology of Diabetes I, et al. Intensive diabetes treatment and cardiovascular disease in patients with type 1 diabetes. *N Engl J Med*. 2005;353:2643–2653. doi: [10.1056/NEJMoa052187](https://doi.org/10.1056/NEJMoa052187)
- Chen L, Magliano DJ, Zimmet PZ. The worldwide epidemiology of type 2 diabetes mellitus—present and future perspectives. *Nat Rev Endocrinol*. 2011;8:228–236. doi: [10.1038/nrendo.2011.183](https://doi.org/10.1038/nrendo.2011.183)
- Deanfield JE, Halcox JP, Rabelink TJ. Endothelial function and dysfunction: testing and clinical relevance. *Circulation*. 2007;115:1285–1295. doi: [10.1161/CIRCULATIONAHA.106.652859](https://doi.org/10.1161/CIRCULATIONAHA.106.652859)
- Wegiel B, Gallo DJ, Raman KG, Karlsson JM, Ozanich B, Chin BY, Tzeng E, Ahmad S, Ahmed A, Baty CJ, et al. Nitric oxide-dependent bone marrow progenitor mobilization by carbon monoxide enhances endothelial repair after vascular injury. *Circulation*. 2010;121:537–548. doi: [10.1161/CIRCULATIONAHA.109.887695](https://doi.org/10.1161/CIRCULATIONAHA.109.887695)
- Hu QS, Chen YX, Huang QS, Deng BQ, Xie SL, Wang JF, Nie RQ. Carbon monoxide releasing molecule accelerates reendothelialization after carotid artery balloon injury in rat. *Biomed Environ Sci*. 2015;28:253–262. doi: [10.3967/bes2015.036](https://doi.org/10.3967/bes2015.036)
- Hu Q, Ke X, Zhang T, Chen Y, Huang Q, Deng B, Xie S, Wang J, Nie R. Hydrogen sulfide improves vascular repair by promoting endothelial nitric oxide synthase-dependent mobilization of endothelial progenitor cells. *J Hypertens*. 2019;37:972–984. doi: [10.1097/HJH.0000000000001983](https://doi.org/10.1097/HJH.0000000000001983)
- Hu Q, Zhang T, Li Y, Feng J, Nie R, Wang X, Peng C, Ke X. beta2AR-dependent signaling contributes to in-vivo reendothelialization capacity of endothelial progenitor cells by shear stress. *J Hypertens*. 2020;38:82–94. doi: [10.1097/HJH.0000000000002203](https://doi.org/10.1097/HJH.0000000000002203)
- Hu Q, Dong X, Zhang K, Song H, Li C, Zhang T, Feng J, Ke X, Li H, Chen Y, et al. Fluid shear stress ameliorates prehypertension-associated decline in endothelium-reparative potential of early endothelial progenitor cells. *J Cardiovasc Transl Res*. 2022;15:1049–1063. doi: [10.1007/s12265-022-10235-y](https://doi.org/10.1007/s12265-022-10235-y)
- Hill JM, Zalos G, Halcox JP, Schenke WH, Waclawiw MA, Quyyumi AA, Finkel T. Circulating endothelial progenitor cells, vascular function, and cardiovascular risk. *N Engl J Med*. 2003;348:593–600. doi: [10.1056/NEJMoa022287](https://doi.org/10.1056/NEJMoa022287)
- Fadini GP, Miorin M, Facco M, Bonamico S, Baesso I, Grego F, Menegolo M, de Kreutzenberg SV, Tiengo A, Agostini C, et al. Circulating endothelial progenitor cells are reduced in peripheral vascular complications of type 2 diabetes mellitus. *J Am Coll Cardiol*. 2005;45:1449–1457. doi: [10.1016/j.jacc.2004.11.067](https://doi.org/10.1016/j.jacc.2004.11.067)
- Sorrentino SA, Bahlmann FH, Besler C, Muller M, Schulz S, Kirchhoff N, Doerries C, Horvath T, Limbourg A, Limbourg F, et al. Oxidant stress impairs in vivo reendothelialization capacity of endothelial progenitor cells from patients with type 2 diabetes mellitus: restoration by the peroxisome proliferator-activated receptor-gamma agonist rosiglitazone. *Circulation*. 2007;116:163–173. doi: [10.1161/CIRCULATIONAHA.106.684381](https://doi.org/10.1161/CIRCULATIONAHA.106.684381)
- Ma W, Zhong T, Chen J, Ke X, Zuo H, Liu Q. Exogenous H(2)S reverses high glucose-induced endothelial progenitor cells dysfunction via regulating autophagy. *Bioengineered*. 2022;13:1126–1136. doi: [10.1080/21655979.2021.2017695](https://doi.org/10.1080/21655979.2021.2017695)

13. Wong GW, Krawczyk SA, Kitidis-Mitrokostas C, Ge G, Spooner E, Hug C, Gimeno R, Lodish HF. Identification and characterization of CTRP9, a novel secreted glycoprotein, from adipose tissue that reduces serum glucose in mice and forms heterotrimers with adiponectin. *FASEB J*. 2009;23:241–258. doi: [10.1096/fj.08-114991](https://doi.org/10.1096/fj.08-114991)
14. Wong GW, Wang J, Hug C, Tsao TS, Lodish HF. A family of Acrp30/adiponectin structural and functional paralogs. *Proc Natl Acad Sci U S A*. 2004;101:10302–10307. doi: [10.1073/pnas.0403760101](https://doi.org/10.1073/pnas.0403760101)
15. Yu XH, Zhang DW, Zheng XL, Tang CK. C1q tumor necrosis factor-related protein 9 in atherosclerosis: mechanistic insights and therapeutic potential. *Atherosclerosis*. 2018;276:109–116. doi: [10.1016/j.atherosclerosis.2018.07.022](https://doi.org/10.1016/j.atherosclerosis.2018.07.022)
16. Zheng Q, Yuan Y, Yi W, Lau WB, Wang Y, Wang X, Sun Y, Lopez BL, Christopher TA, Peterson JM, et al. C1q/TNF-related proteins, a family of novel adipokines, induce vascular relaxation through the adiponectin receptor-1/AMPK/eNOS/nitric oxide signaling pathway. *Arterioscler Thromb Vasc Biol*. 2011;31:2616–2623. doi: [10.1161/ATVBAHA.111.231050](https://doi.org/10.1161/ATVBAHA.111.231050)
17. Uemura Y, Shibata R, Ohashi K, Enomoto T, Kambara T, Yamamoto T, Ogura Y, Yuasa D, Joki Y, Matsuo K, et al. Adipose-derived factor CTRP9 attenuates vascular smooth muscle cell proliferation and neointimal formation. *FASEB J*. 2013;27:25–33. doi: [10.1096/fj.12-213744](https://doi.org/10.1096/fj.12-213744)
18. Huang C, Zhang P, Li T, Li J, Liu T, Zuo A, Chen J, Guo Y. Overexpression of CTRP9 attenuates the development of atherosclerosis in apolipoprotein E-deficient mice. *Mol Cell Biochem*. 2019;455:99–108. doi: [10.1007/s11010-018-3473-y](https://doi.org/10.1007/s11010-018-3473-y)
19. Ahmed SF, Shabayek MI, Abdel Ghany ME, El-Hefnawy MH, El-Mesallamy HO. Role of CTRP3, CTRP9 and MCP-1 for the evaluation of T2DM associated coronary artery disease in Egyptian postmenopausal females. *PLoS One*. 2018;13:e0208038. doi: [10.1371/journal.pone.0208038](https://doi.org/10.1371/journal.pone.0208038)
20. Si Y, Fan W, Sun L. A review of the relationship between CTRP family and coronary artery disease. *Curr Atheroscler Rep*. 2020;22:22. doi: [10.1007/s11883-020-00840-0](https://doi.org/10.1007/s11883-020-00840-0)
21. Yamaguchi S, Shibata R, Ohashi K, Enomoto T, Ogawa H, Otaka N, Hiramatsu-Ito M, Masutomi T, Kawarishi H, Murohara T, et al. C1q/TNF-related protein 9 promotes revascularization in response to ischemia via an eNOS-dependent manner. *Front Pharmacol*. 2020;11:1313. doi: [10.3389/fphar.2020.01313](https://doi.org/10.3389/fphar.2020.01313)
22. Sun H, Zhu X, Zhou Y, Cai W, Qiu L. C1q/TNF-related Protein-9 ameliorates ox-LDL-induced endothelial dysfunction via PGC-1 α /AMPK-mediated antioxidant enzyme induction. *Int J Mol Sci*. 2017;18:1097. doi: [10.3390/ijms18061097](https://doi.org/10.3390/ijms18061097)
23. Hardie DG, Carling D, Carlson M. The AMP-activated/SNF1 protein kinase subfamily: metabolic sensors of the eukaryotic cell? *Annu Rev Biochem*. 1998;67:821–855. doi: [10.1146/annurev.biochem.67.1.821](https://doi.org/10.1146/annurev.biochem.67.1.821)
24. Kahn BB, Alquier T, Carling D, Hardie DG. AMP-activated protein kinase: ancient energy gauge provides clues to modern understanding of metabolism. *Cell Metab*. 2005;1:15–25. doi: [10.1016/j.cmet.2004.12.003](https://doi.org/10.1016/j.cmet.2004.12.003)
25. Garcia-Prieto CF, Gil-Ortega M, Aranguex I, Ortiz-Besoain M, Somoza B, Fernandez-Alfonso MS. Vascular AMPK as an attractive target in the treatment of vascular complications of obesity. *Vascul Pharmacol*. 2015;67-69:10–20. doi: [10.1016/j.vph.2015.02.017](https://doi.org/10.1016/j.vph.2015.02.017)
26. Garcia-Prieto CF, Gil-Ortega M, Plaza A, Manzano-Lista FJ, Gonzalez-Blazquez R, Alcalá M, Rodríguez-Rodríguez P, Viana M, Aranguex I, Gollasch M, et al. Caloric restriction induces H(2)O(2) formation as a trigger of AMPK-eNOS-NO pathway in obese rats: role for CAMKII. *Free Radic Biol Med*. 2019;139:35–45. doi: [10.1016/j.freeradbiomed.2019.05.016](https://doi.org/10.1016/j.freeradbiomed.2019.05.016)
27. Garcia-Prieto CF, Pulido-Olmo H, Ruiz-Hurtado G, Gil-Ortega M, Aranguex I, Rubio MA, Ruiz-Gayo M, Somoza B, Fernandez-Alfonso MS. Mild caloric restriction reduces blood pressure and activates endothelial AMPK-Pi3K-Akt-eNOS pathway in obese Zucker rats. *Vascul Pharmacol*. 2015;65:3–12. doi: [10.1016/j.vph.2014.12.001](https://doi.org/10.1016/j.vph.2014.12.001)
28. Prieto D, Contreras C, Sanchez A. Endothelial dysfunction, obesity and insulin resistance. *Curr Vasc Pharmacol*. 2014;12:412–426. doi: [10.2174/157016112666140423221008](https://doi.org/10.2174/157016112666140423221008)
29. Cohen KE, Katunaric B, Schulz ME, SenthilKumar G, Young MS, Mace JE, Freed JK. Role of adiponectin receptor 1 in promoting nitric oxide-mediated flow-induced dilation in the human microvasculature. *Front Pharmacol*. 2022;13:875900. doi: [10.3389/fphar.2022.875900](https://doi.org/10.3389/fphar.2022.875900)
30. Ferreri DM, Minnear FL, Yin T, Kowalczyk AP, Vincent PA. N-cadherin levels in endothelial cells are regulated by monolayer maturity and p120 availability. *Cell Commun Adhes*. 2008;15:333–349. doi: [10.1080/15419060802440377](https://doi.org/10.1080/15419060802440377)
31. Hu Q, Guo Y, Zhang T, Feng J, Wang J, Dong X, Chen Y, Nie R, Feng Z, Huang Y, et al. Importance of beta(2)AR elevation for re-endothelialization capacity mediated by late endothelial progenitor cells in hypertensive patients. *Am J Physiol Heart Circ Physiol*. 2021;320:H867–H880. doi: [10.1152/ajpheart.00596.2020](https://doi.org/10.1152/ajpheart.00596.2020)
32. Nelson J, Wu Y, Jiang X, Berretta R, Houser S, Choi E, Wang J, Huang J, Yang X, Wang H. Hyperhomocysteinemia suppresses bone marrow CD34+/VEGF receptor 2+ cells and inhibits progenitor cell mobilization and homing to injured vasculature—a role of beta1-integrin in progenitor cell migration and adhesion. *FASEB J*. 2015;29:3085–3099. doi: [10.1096/fj.14-267989](https://doi.org/10.1096/fj.14-267989)
33. Charan J, Kantharia ND. How to calculate sample size in animal studies? *J Pharmacol Pharmacother*. 2013;4:303–306. doi: [10.4103/0976-500X.119726](https://doi.org/10.4103/0976-500X.119726)
34. Asahara T, Murohara T, Sullivan A, Silver M, van der Zee R, Li T, Witzenbichler B, Schatteman G, Isner JM. Isolation of putative progenitor endothelial cells for angiogenesis. *Science*. 1997;275:964–967. doi: [10.1126/science.275.5302.964](https://doi.org/10.1126/science.275.5302.964)
35. Hur J, Yoon CH, Kim HS, Choi JH, Kang HJ, Hwang KK, Oh BH, Lee MM, Park YB. Characterization of two types of endothelial progenitor cells and their different contributions to neovascularogenesis. *Arterioscler Thromb Vasc Biol*. 2004;24:288–293. doi: [10.1161/01.ATV.0000114236.77009.06](https://doi.org/10.1161/01.ATV.0000114236.77009.06)
36. Aicher A, Heeschen C, Mildner-Rihm C, Urbich C, Ihling C, Technau-Ihling K, Zeiher AM, Dimmeler S. Essential role of endothelial nitric oxide synthase for mobilization of stem and progenitor cells. *Nat Med*. 2003;9:1370–1376. doi: [10.1038/nm948](https://doi.org/10.1038/nm948)
37. Everaert BR, Van Craenenbroeck EM, Hoymans VY, Haine SE, Van Nassauw L, Conraads VM, Timmermans JP, Vrints CJ. Current perspective of pathophysiological and interventional effects on endothelial progenitor cell biology: focus on PI3K/AKT/eNOS pathway. *Int J Cardiol*. 2010;144:350–366. doi: [10.1016/j.ijcard.2010.04.018](https://doi.org/10.1016/j.ijcard.2010.04.018)
38. Chen YH, Lin SJ, Lin FY, Wu TC, Tsao CR, Huang PH, Liu PL, Chen YL, Chen JW. High glucose impairs early and late endothelial progenitor cells by modifying nitric oxide-related but not oxidative stress-mediated mechanisms. *Diabetes*. 2007;56:1559–1568. doi: [10.2337/db06-1103](https://doi.org/10.2337/db06-1103)
39. Huang PH, Chen JS, Tsai HY, Chen YH, Lin FY, Leu HB, Wu TC, Lin SJ, Chen JW. Globular adiponectin improves high glucose-suppressed endothelial progenitor cell function through endothelial nitric oxide synthase dependent mechanisms. *J Mol Cell Cardiol*. 2011;51:109–119. doi: [10.1016/j.yjmcc.2011.03.008](https://doi.org/10.1016/j.yjmcc.2011.03.008)
40. Yan W, Guo Y, Tao L, Lau WB, Gan L, Yan Z, Guo R, Gao E, Wong GW, Koch WL, et al. C1q/tumor necrosis factor-related Protein-9 regulates the fate of implanted mesenchymal stem cells and mobilizes their protective effects against ischemic heart injury via multiple novel signaling pathways. *Circulation*. 2017;136:2162–2177. doi: [10.1161/CIRCULATIONAHA.117.029557](https://doi.org/10.1161/CIRCULATIONAHA.117.029557)
41. Hu Q, Zhang B, Liu Y, Guo Y, Zhang T, Nie R, Ke X, Dong X. The effect of fluid shear stress in hydrogen sulphide production and cystathionine gamma-lyase expression in human early endothelial progenitor cells. *Ann Transl Med*. 2020;8:1318. doi: [10.21037/atm-20-6467](https://doi.org/10.21037/atm-20-6467)
42. Galasso G, De Rosa R, Ciccarelli M, Sorriento D, Del Giudice C, Strisciuglio T, De Biase C, Luciano R, Piccolo R, Pierri A, et al. beta2-adrenergic receptor stimulation improves endothelial progenitor cell-mediated ischemic neoangiogenesis. *Circ Res*. 2013;112:1026–1034. doi: [10.1161/CIRCRESAHA.111.300152](https://doi.org/10.1161/CIRCRESAHA.111.300152)
43. Vasa M, Fichtlscherer S, Aicher A, Adler K, Urbich C, Martin H, Zeiher AM, Dimmeler S. Number and migratory activity of circulating endothelial progenitor cells inversely correlate with risk factors for coronary artery disease. *Circ Res*. 2001;89:E1–E7. doi: [10.1161/hh1301.093953](https://doi.org/10.1161/hh1301.093953)
44. Du XL, Edelstein D, Dimmeler S, Ju Q, Sui C, Brownlee M. Hyperglycemia inhibits endothelial nitric oxide synthase activity by posttranslational modification at the Akt site. *J Clin Invest*. 2001;108:1341–1348. doi: [10.1172/JCI11235](https://doi.org/10.1172/JCI11235)
45. Salt IP, Morrow VA, Brandie FM, Connell JM, Petrie JR. High glucose inhibits insulin-stimulated nitric oxide production without reducing endothelial nitric-oxide synthase Ser1177 phosphorylation in human aortic endothelial cells. *J Biol Chem*. 2003;278:18791–18797. doi: [10.1074/jbc.M210618200](https://doi.org/10.1074/jbc.M210618200)
46. Ke X, Shu XR, Wu F, Hu QS, Deng BQ, Wang JF, Nie RQ. Overexpression of the beta2AR gene improves function and re-endothelialization

- capacity of EPCs after arterial injury in nude mice. *Stem Cell Res Ther.* 2016;7:73. doi: [10.1186/s13287-016-0335-y](https://doi.org/10.1186/s13287-016-0335-y)
47. Morrow VA, Fougelle F, Connell JM, Petrie JR, Gould GW, Salt IP. Direct activation of AMP-activated protein kinase stimulates nitric-oxide synthesis in human aortic endothelial cells. *J Biol Chem.* 2003;278:31629–31639. doi: [10.1074/jbc.M212831200](https://doi.org/10.1074/jbc.M212831200)
 48. Kadowaki T, Yamauchi T. Adiponectin and adiponectin receptors. *Endocr Rev.* 2005;26:439–451. doi: [10.1210/er.2005-0005](https://doi.org/10.1210/er.2005-0005)
 49. Heiker JT, Kosel D, Beck-Sickingler AG. Molecular mechanisms of signal transduction via adiponectin and adiponectin receptors. *Biol Chem.* 2010;391:1005–1018. doi: [10.1515/BC.2010.104](https://doi.org/10.1515/BC.2010.104)
 50. Buechler C, Wanninger J, Neumeier M. Adiponectin receptor binding proteins—recent advances in elucidating adiponectin signalling pathways. *FEBS Lett.* 2010;584:4280–4286. doi: [10.1016/j.febslet.2010.09.035](https://doi.org/10.1016/j.febslet.2010.09.035)
 51. Madonna R, Montebello E, Lazzarini G, Zurro M, De Caterina R. NA⁺/H⁺ exchanger 1- and aquaporin-1-dependent hyperosmolarity changes decrease nitric oxide production and induce VCAM-1 expression in endothelial cells exposed to high glucose. *Int J Immunopathol Pharmacol.* 2010;23:755–765. doi: [10.1177/039463201002300309](https://doi.org/10.1177/039463201002300309)
 52. Madonna R, Pieragostino D, Rossi C, Confalone P, Cicalini I, Minnucci I, Zucchelli M, Del Boccio P, De Caterina R. Simulated hyperglycemia impairs insulin signaling in endothelial cells through a hyperosmolar mechanism. *Vascul Pharmacol.* 2020;130:106678. doi: [10.1016/j.vph.2020.106678](https://doi.org/10.1016/j.vph.2020.106678)
 53. Yoder MC. Human endothelial progenitor cells. *Cold Spring Harb Perspect Med.* 2012;2:a006692. doi: [10.1101/cshperspect.a006692](https://doi.org/10.1101/cshperspect.a006692)
 54. Chen D, Weng L, Chen C, Zheng J, Wu T, Zeng S, Zhang S, Xiao J. Inflammation and dysfunction in human aortic endothelial cells associated with poly-L-lactic acid degradation in vitro are alleviated by curcumin. *J Biomed Mater Res A.* 2019;107:2756–2763. doi: [10.1002/jbm.a.36778](https://doi.org/10.1002/jbm.a.36778)